

## Notes

Detailed description for PFT specific features and parameters are found in the following papers.

|             |   |                          |
|-------------|---|--------------------------|
| BoND        | (Boreal Needle-leaved Deciduous PFT):           | Sato et al. (2009)       |
| TrBE1~4     | (Tropical Broad-leaved Evergreen PFTs, Asian):  | Sato (2009)              |
| TrBE5       | (Tropical Broad-leaved Evergreen PFT, African): | Sato and Ise (submitted) |
| TrBR        | (Tropical Broad-leaved Rain green PFT):         | Sato and Ise (submitted) |
| TrH         | (C4-type photosynthesis grass):                 | Sato and Ise (submitted) |
| Other PFTs: |   | Sato et al. (2007)       |

TrBE5 can only establish in African continent. In African continent, only TrBE5 and TrBR are allowed to establish for woody PFT.

## Overview

The simulation unit of the SEIB–DGVM is a  $30 \times 30$ -m spatially explicit virtual forest (size of virtual forest is specified by a parameter, *Max\_loc*), in which individual trees establish, compete, and die. Grass layer cells, which divides forest floor by  $10 \times 10$ , also exists in the forest under the tree canopy. Appendix B1 shows the input and output of the model. Appendix B2 summarizes the processes represented, which can be classified into three groups: physical, physiological, and vegetation dynamics. The SEIB–DGVM utilizes three computational time steps: a daily time step for all physical and physiological processes, and an annual time step for vegetation dynamics and disturbance. Appendix B3 lists the symbols used in the model's equations. Those that begin with a capital letter are constants, while those that begin with a lowercase letter are variables. Plant species are classified into small number of plant functional types (PFTs) to enable global-scale simulation (Table 1). These PFTs can coexist in the same simulation plot.

## Plant properties

Woody PFTs are represented by individual trees composed of three organs: the crown and the trunk, both of which are cylindrical, and the fine roots, which are formless (Fig. 1). The crown is defined by biomass ( $mass_{leaf}$ ), leaf area ( $la$ ), diameter ( $crown_{diameter}$ ), and depth ( $crown_{depth}$ ); the trunk, by biomass ( $mass_{trunk}$ ), height ( $height$ ), and the diameters of sapwood ( $dbh_{sapwood}$ ) and heartwood ( $dbh_{heartwood}$ ); the fine roots, by biomass ( $mass_{root}$ ) only. Trunk biomass ( $mass_{trunk}$ ) includes both branch and coarse root biomass. Besides these variables, each individual tree has a reserve resource ( $mass_{stock}$ ), which is used for foliation after the dormant phase (for deciduous PFTs) and after fires. Grass PFTs are represented in a much simpler way, consisting of leaf, root, and a reserve resource, all of which are represented by biomass per unit area ( $gmass_{leaf}$ ,  $gmass_{root}$ , and  $gmass_{stock}$ , respectively). Grass layer divides forest floor by  $10 \times 10$  (A parameter *DivedG* specifies this resolution). While each grass cell in a virtual forest shares common pool of soil water, it receives distinct intensity of sun light, which is calculated by considering horizontal distribution of tree leaves.

## Carbon cycles

Figure 2 provides an overview of the carbon cycle as represented in the SEIB–DGVM. Atmospheric  $CO_2$  is assimilated by the foliage of woody PFTs and grass PFTs. This assimilated carbon is then transferred to all of the other organs, where maintenance and growth respiration occurs. All respired carbon is recycled to the atmosphere as  $CO_2$ . At the same time, defoliation at the end of the growing season, turnover of leaves and fine roots, and tree death produce litter, which is added to the litter pool. When the litter pool decomposes, some portion of the carbon within it is recycled to the atmosphere, while the remaining carbon is added to pools of soil organic carbon 1 (fast decomposition rate) or 2 (slow decomposition rate). Finally, decomposed soil organic carbon is recycled to the atmosphere as  $CO_2$ .

## Water cycles

Figure 3 provides an overview of the water cycle as represented in the model. The ground is composed of 30 soil layers, of which depth is equally 0.1m. Hydrological and radiation properties of soil is given by four grid-specific parameters, *ALBEDO*, *Wsat*, *Wfi*, and *Wwilt*. Each parameter indicates soil albedo, soil moisture at saturation point, field capacity, and wilting point, respectively. Values for these parameters are taken from soil texture data in BIOME3 (Haxeltine and Prentice 1996), which is based on the FAO soil data set (Zobler

1986) (FAO 1991). Water can be pooled as snow ( $pool_{snow}$ ) and as water in soil layers  $i$  ( $pool_{w(i)}$ ). Soil liquid surface water that is not infiltrated within a day is immediately removed as runoff.

### Daily water flow (in the order of computation)

Precipitation ( $prec$ ) is divided into rainfall ( $prec_{rain}$ ) and snowfall ( $prec_{snow}$ ) using empirical function of the daily mean temperature of air ( $tmp_{air}$ ) (Ito and Oikawa, 2002):

$$prec_{snow} = prec / [ 1 + \exp( 0.75 \times tmp_{air} - 1.5 ) ] \quad (1)$$

$$prec_{rain} = prec - prec_{snow}. \quad (2)$$

Snowfall is added to the snow pool ( $pool_{snow}$ ), which melts as a function of temperature at top soil layer ( $tmp_{soil(1)}$ ):

$$\Delta pool_{snow} = prec_{snow} - tw \quad (3)$$

$$tw = pool_{snow} / [ 1 + \exp ( -0.3 ( tmp_{soil(1)} - 10 ) ) ], \quad (4)$$

where  $tw$  is daily snow melting water. A portion of the rainfall is caught by leaves, and evaporates before reaching the soil surface. The fraction of this intercepted rainfall is a function of leaf area index ( $lai$  in  $m^2 m^{-2}$ ).

$$ic = \min [ prec_{rain} , 3.0 \times rain \times ( 1.0 - \exp(-1.0 \times lai) ) ], \quad (5)$$

where  $rain$  is expected number of rain in a day, which is calculated using method in Neilson(1995). From the above equations, the daily liquid water to reach the soil surface can be obtained as  $prec_{rain} + tw - ic$ .

### Daily changes of the soil water storages (in the order of computation)

Daily input of liquid water on the ground surface will penetrate into the top soil layer until fulfill its saturation point, if temperature at top soil layer is more than 0°C. The remaining water immediately washes off the surface as runoff. For each soil layer, soil water above field

capacity percolates to the next soil layer until fulfills its saturation point, while the remaining stays in current layer. This soil water movement is inhibited when soil temperature at the current or next layer is less than zero. Soil water in bottom soil layer cannot penetrate or runoff. Plants can absorb soil water from unfrozen top  $RootDepth$  soil layers ( $10 \times RootDepth$  cm depth) until these wilting points, and they transpire absorbed water. Here,  $RootDepth$  is a PFT specific parameter. Evaporation occurs only from water at top 5 soil layer (0-50cm depth). Daily amounts of transpiration and evaporation were calculated using Penman–Monteith equation {Monteith, 1990 #584} (see Appendix A6 for detail).

To control leaf phenology and the rate of photosynthesis as a function of soil water availability, the physiological status of water availability is defined for each PFT ( $stat_{water}$ , 0.0–1.0) as follows:

$$stat_{water} = \frac{\text{sum}(pool_{w(1)}, pool_{w(2)}, \dots, pool_{w(RootDepth)}) / Depth / RootDepth - W_{wilt}}{W_{fi} - W_{wilt}}. \text{ (Default)}$$

$$stat_{water} = \frac{\text{max}(pool_{w(1)}, pool_{w(2)}, \dots, pool_{w(RootDepth)}) / Depth - W_{wilt}}{W_{fi} - W_{wilt}}. \text{ (for BoNS)}$$

Soil layers, whose temperature is than 0 °C, are omitted for this calculation. And if temperature of all soil layers within the  $RootDepth$ ,  $stat_{water}$  is assumed to be zero.

#### Establishment of Woody PFTs

In the model, new individual trees establish on the last day of each simulation year. It is assumed that establishment only occurs if total precipitation of the current year (in mm) exceeds 20 times the annual mean temperature (in °C) (Köppen, 1936). Each woody PFT has distinct of climatic range for establishment, following the LPJ–DGVM (Sitch et al., 2003): the maximum coldest-month temperature ( $TC_{max}$ ), and the minimum growing-degree day ( $GDD_{min}$ ), as shown in Appendix B5. Both climatic limitations are applied to the running means of the last 20 years.

For some PFTs, we assumed that they can only establish when the midday photosynthetically active radiation (PAR, hereafter) that is computed for each 1×1-m grid cell on the surface of

the grass layer and averaged for the previous year exceeded  $PAR_{min}$   $\mu\text{mol photon m}^{-2} \text{s}^{-1}$ . For some PFTs, we additionally assumed that they cannot establish when drought month (monthly potential evapotranspiration is more than monthly actual precipitation) existed more than  $DM_{max}$  month in the previous year. For BoNS, we assumed that establishment can only occur during 50 years from forest fire.

For reproducing geographical distribution of woody PFTs in African continent, we calibrated bioclimatic limits as follows. TrBE5 and TrBR can only establish if number of dry month in the previous year is more than 4 and 9 month, respectively. Here, dry month is determined for the month whose precipitation is less than potential evapotranspiration that is calculated by Priestley-Taylor model with coefficient 1.26 (Rosenberg et al. 1983)

All newly established trees have 0.01 m of  $dbh_{sapwood}$ , 0.00 m of  $dbh_{heartwood}$ , and 0 m of lowest-branch height (i.e.,  $height = crown_{depth}$ ). From these properties, tree height ( $height$ ), crown diameter ( $crown_{diameter}$ ), and stem biomass ( $mass_{trunk}$ ) are calculated using allometric and allocation formulas described in the section titled 'Tree growth.' These newly established trees initially lack leaves and fine roots, but have 500 g DM of reserve resource ( $mass_{stock}$ ). The biomass of newly established trees is taken from the litter pool of the same forest so that total carbon storage of the forest remains the same.

The floor of the virtual forest is divided into a grid of  $1.0 \times 1.0$ -m mesh (A parameter *Dived* specifies this resolution), and each tree monopolizes one of the mesh boxes. The SEIB-DGVM assumes that crowns of different trees cannot occupy the same space, and thus mesh boxes in which a newly established tree interacts with existing trees are not available for further establishment. For each available mesh box, the same establishment rate,  $P_{establish}$ , was assumed.

There are 4 scenarios to allocate available mesh box to woody PFT that can establish under the given climate. Note, for changing establishment scenario, modify *Est\_scenario* in the parameter file.

**Scenario 1** (one specific PFT establish): only one woody PFT, which is specified by *Est\_pft\_OnOff* in the parameter file, can monopolize available mesh box.

**Scenario 2** (infinite seed dispersal): every woody PFTs that can establish at the given climatic conditions share available mesh box equally.

**Scenario 3** (no seed dispersal): Same as scenario 2 until specific year *Est\_year\_change* in the parameter file. After that, allocate available mesh box among each woody PFTs in proportion to existing biomass at the forest stand.

**Scenario 4** (Scenario 3 + long migrated seed): Same as scenario 2 until year *Est\_year\_change*. After that time, available boxes are allocated to deterministic and stochastic establishment components in proportion to  $1.0 - Est_{Random}$  and  $Est_{Random}$ , respectively. Here,  $Est_{Random}$  determines fraction of establishment cells allocated to stochastic establishment. The deterministic establishment only occurs when mean biomass of woody PFT in the virtual forest was more than 100g dry mass (DM)  $m^{-2}$ : It implies that we assumed that the deterministic establishment only occurs when certain amount of seed production is expected in the virtual forest: Available mesh boxes for deterministic establishment were allocated in proportion to the biomass of each woody PFT. Available mesh boxes for stochastic establishment were equally allocated to all woody PFTs those have capability to establish under the given environment.

#### Establishment of Grass PFTs

For grass PFTs, establishment processes are not treated explicitly. A small amount of grass 'seed' is always assumed to be present, even if the environment is unfavorable to grass survival; densities of grass biomass ( $gmass_{leaf}$ ,  $gmass_{root}$ , and  $gmass_{stock}$ ) never decrease below their minimum limits (0.1 g  $m^{-2}$  for all).

The floor of the virtual forest is monopolized by one of the two grass PFTs, namely C<sub>3</sub> and C<sub>4</sub> grass. On the end of each year, dominant grass type is determined as follows: For each grass growing month (mean air temperature is more than 5.0 C °, and precipitation is more than 25mm/month), advantageous grass type is decided. C<sub>4</sub> grass type is advantageous if monthly mean air temperature is more than  $1.0 / (1.0/(x-10.0) + 1/68.0)$ , where  $x$  is partial pressure of atmospheric CO<sub>2</sub> (Pa). C<sub>3</sub> grass type is advantageous in other cases. This equation was estimated from figure 1b of Collatz et al. (1998). If C<sub>4</sub> advantageous month is larger than for C<sub>3</sub> advantageous month, C<sub>4</sub> grass type will be dominant in the following year, and vice versa.

When the dominant PFT changes, the biomass properties ( $gmass_{leaf}$ ,  $gmass_{root}$ , and  $gmass_{stock}$ ) of the two grass PFTs are exchanged so that the total grass biomass of the plot remains the same.

### PAR Allocation

For each simulation day, the radiation module of the SEIB-DGVM calculates direct and diffuse components of photosynthetically active radiation at midday ( $par_{direct}$  and  $par_{diffuse}$ , respectively) (see Appendix A2 for the calculation). How these PARs are distributed among trees and grass primarily controls plant growth and competition.

### Woody PFTs

Each tree crown is horizontally sliced into 10-cm-deep 'disks,' for which photosynthesis is calculated separately (Fig. 1). The midday PAR that enters disk  $l$  of individual  $n$ ,  $par_{wood(l,n)}$ , is calculated as follows, where  $fpar_{direct(l,n)}$  and  $fpar_{diffuse(l)}$  represent the relative intensity of direct and diffuse PAR of disk  $l$  of tree  $n$  compared to the forest top, respectively:

$$par_{wood(l,n)} = fpar_{direct(l,n)} \times par_{direct} + fpar_{diffuse(l)} \times par_{diffuse}. \quad (10)$$

To obtain  $fpar_{direct(l,n)}$ , a virtual cylinder with a cross section equal to disk  $l$ , was extended from the disk to the direction of the south with angle  $0.86 \times sl_{hgt}$ , where  $sl_{hgt}$  is midday solar angle (Fig. 4). The horizontal line of  $0.86 \times sl_{hgt}$  equally divides daily sum of solar radiation into two, when daily changes of solar angle and solar radiation are  $\sin$  and  $\sin^2$ , respectively. Then, the total leaf area falling within the cylinder,  $fpar_{direct(l,n)}$ , was summed using Beer's law as follows, where  $la_{(p)}$  (in  $m^2$ ) is the sum of the leaf area of PFT  $p$  within the cylinder,  $crown_{area(n)}$  is the cross section of the crown area of tree  $n$ , and  $EK_{(p)}$  is the vertical light attenuation coefficient of PFT  $p$ :

$$fpar_{direct(l,n)} = \exp\left(\frac{-1.0 \times \sum_{p=1}^{woody\_pft} (EK_{(p)} \times la_{(p)})}{crown_{area(n)}}\right). \quad (11)$$

In this calculation, the virtual forest was assumed to repeat; i.e., if the cylinder exited the forest edge at a lower position than the tallest tree, the cylinder would reenter the forest from

the opposite edge at the same position in a west–east vertical plane. The calculation of  $fpar_{direct(l,n)}$  is the most computationally power-consuming process in the model. Thus, this factor is updated in 14-day intervals.

Because diffuse PAR scatters in the sky, we ignored horizontal structures in the forest while calculating its distribution in the forest; all disks at the same height receive the same intensity of diffuse PAR. The relative intensity of diffuse PAR on the disk layer  $l$ ,  $fpar_{diffuse(l)}$ , is calculated every day as follows, where  $lai_{(l,p)}$  is the leaf area index (in  $m^2 m^{-2}$ ), which is calculated only for PFT  $p$  and for leaves above disk layer  $l$ :

$$fpar_{diffuse(l)} = \exp\left(-1.0 \times \sum_{p=1}^{woody\_pft} (EK_{(p)} \times lai_{(l,p)})\right). \quad (12)$$

### Grass PFTs

The midday PAR that reaches the grass cell  $i$   $par_{grass(i)}$  is calculated every day as follows, where  $lai_{(p,i)}$  is the leaf area index of woody PFT  $p$  in grass cell  $i$ :

$$par_{grass(i)} = (par_{direct} + par_{diffuse}) \times \exp\left(-1.0 \times \sum_{p=1}^{woody\_pft} (eK_{(p)} \times lai_{(p,i)})\right). \quad (13)$$

As shown in the equation below,  $eK_{(p)}$  is the light attenuation coefficient for the direction of the sun at midday. It is calculated every day as a function of solar angle at midday  $sl_{hgt}$  (see Appendix A2 for the calculation) and the light attenuation coefficient for vertical direction  $EK_{(p)}$ :

$$eK_{(p)} = EK_{(p)} / \{0.86 \sin(sl_{hgt})\}. \quad (14)$$

The horizontal line of  $0.86 \times sl_{hgt}$  equally divides daily sum of solar radiation into two, when daily changes of solar angle and solar radiation are  $\sin$  and  $\sin^2$ , respectively.

### Photosynthesis

To compute photosynthesis, the SEIB–DGVM assumes that environmental conditions other than PAR intensity (e.g. air temperature,  $CO_2$ , and water) are equal among all the leaves, all



day. The single-leaf photosynthetic rate is formulated as a simple Michaelis-type function of the intensity of PAR,  $par$ :

$$p_{single} = \frac{p_{sat} \times lue \times par}{p_{sat} + lue \times par} \quad (15)$$

, where  $p_{sat}$  and  $lue$  are the light-saturated photosynthetic rate and light-use efficiency, respectively (see Appendix A4 for the calculation).

### Woody PFTs

According to Kuroiwa (1979), a daily change in PAR can be approximated by a sine square function as follows, where  $dlen$  is day length (hour), and  $x$  and  $par_l$  are intensity of PAR on crown disk  $l$  at time  $t$  (hour from sunrise) and at midday, respectively:

$$x = par_l \times \sin^2\left(\pi \times \frac{t}{dlen}\right). \quad (16)$$

By combining equations 16 and 15, and integrating the resultant equation into day length, the daily photosynthetic production on crown disk  $l$ ,  $gpp_l$ , is obtained as follows, where constant  $12 \cdot 10^{-6} \cdot 3600 / 0.41505$  is the unit converter from [ $\mu\text{mol CO}_2 \text{ m}^{-2} \text{ s}^{-1}$ ] to [ $\text{g DM m}^{-2} \text{ hour m}^{-2} \text{ s}^{-1}$ ] and  $la_l$  is the leaf area within crown disk  $l$ :

$$\begin{aligned} gpp_l &= 12 \times 10^{-6} \times 3600 \times \frac{1}{0.41505} \times la_l \times \int_0^{dlen} p_{single} dt \\ &= 0.090936 \times la_l \times dlen \times p_{sat} \times \left(1 - \frac{1}{\sqrt{1 + lue \times par_l / p_{sat}}}\right). \end{aligned} \quad (17)$$

Using 17, the daily photosynthetic production is obtained for each crown disk of each individual. These values are summed for each individual tree, and then added to the available resource of the tree,  $mass_{available}$ .

### Grass PFTs

Grass leaves are assumed to be uniformly distributed within the grass cell. Thus, PAR of time  $t$  (hour from sunrise) at cumulative grass LAI  $y$  ( $\text{m}^2 \text{m}^{-2}$ ) is calculated as follows, where  $par_{grass(i)}$  is PAR at the surface of the grass cell  $i$  at midday:

$$x_{(i)} = par_{grass(i)} \times \sin^2\left(\pi \frac{t}{dlen}\right) \times e^{-eK \times y}. \quad (18)$$

By combining equations 18 and 15, and integrating the resultant equation into  $t$  and  $y$ , the daily gross primary production of the grass cell  $i$ ,  $gpp_{g(i)}$ , is calculated as follows (Kuroiwa, 1979), where  $lai_{g(i)}$  is the leaf area index of the grass cell  $i$  ( $\text{m}^2 \text{m}^{-2}$ ):

$$\begin{aligned} gpp_{g(i)} &= 0.090936 \times \int_{y=0}^{lai_g} \int_{t=0}^{dlen} p_{single} dt dy \\ &= 0.090936 \times \frac{2 \times dlen \times p_{sat}}{eK} \times \ln \left( \frac{1 + \sqrt{1 + \frac{par_{grass(i)} \times eK \times lue}{p_{sat}}}}{1 + \sqrt{1 + \frac{par_{grass(i)} \times eK \times lue}{p_{sat}} e^{-eK \times lai_g(i)}}} \right). \end{aligned} \quad (19)$$

The daily photosynthetic production is added to available resource of grass cell  $i$ ,  $gmass_{available(i)}$ .

### Canopy Conductance

To compute single-leaf stomatal conductance  $gs$ , the SEIB–DGVM adopts a semi empirical model by Ball et al. (1987), modified by Leuning (1995), where  $co2_{atm}$  is atmospheric  $\text{CO}_2$  concentration,  $co2_{cmp}$  is the  $\text{CO}_2$  compensation point, and  $vpd$  is the vapor pressure deficit between saturated and actual vapor pressures:

$$gs = GS_{b1} + \frac{GS_{b2} \times p_{single}}{(co2_{atm} - co2_{cmp})(1 + vpd / GS_{b3})}. \quad (20)$$

Here,  $GS_{b1}$ ,  $GS_{b2}$ , and  $GS_{b3}$  are PFT-specific parameters. In the model,  $vpd$ ,  $co2_{atm}$ , and  $co2_{cmp}$

are updated every day, according to Appendix A1 and A4. For each crown disk  $l$  of each tree  $n$ , mean daytime stomatal conductance ( $gs_{mean(l,n)}$  in  $\text{mol H}_2\text{O m}^{-2} \text{s}^{-1}$ ) is obtained by combining equations 15, 16, and 20, and integrating the resultant equation into time  $t$ , averaged over the daytime:

$$gs_{mean(l,n)} = GS_{b1} + \frac{GS_{b2} \times p_{sat}}{(co2_{atm} - co2_{cmp})(1 + vpd / GS_{b3})} \left( 1 - \frac{1}{\sqrt{1 + lue \times par_{(l,n)} / p_{sat}}} \right) \quad (21)$$

Thus, mean daytime and whole forest stomatal conductance of woody PFTs,  $ccon_{wood}$  (in  $\text{mol H}_2\text{O m}^{-2} \text{s}^{-1}$ ), is calculated as follows, where  $AREA$  is the area of the simulation plot ( $\text{m}^2$ ):

$$ccon_{wood} = \sum_n \sum_l (gs_{mean(l,n)} \times la_{(l,n)}) / AREA. \quad (22)$$

The mean daytime stomatal conductance for grass PFTs,  $ccon_{grass}$  (in  $\text{mol H}_2\text{O m}^{-2} \text{s}^{-1}$ ), is obtained by combining equations 15, 18, and 20, and integrating the resultant equation into daytime and cumulative LAI.

$$ccon_{grass} = GS_{b1} \times lai_g + \frac{GS_{b2} \times p_{sat}}{(co2_{atm} - co2_{cmp})(1 + vpd / GS_{b3})} \times \frac{2}{eK} \times \ln \left( \frac{1 + \sqrt{1 + \frac{par_{grass} \times eK \times lue}{p_{sat}}}}{1 + \sqrt{1 + \frac{par_{grass} \times eK \times lue}{p_{sat}}} e^{-eK \times lai_g}} \right) \quad (23)$$

$ccon_{grass}$  is calculated for each grass cell, and averaged for the plot. We defined the sum of  $ccon_{wood}$  and  $ccon_{grass}$  as the mean daytime stomatal conductance of this plot ( $ccon$  in  $\text{mol H}_2\text{O m}^{-2} \text{s}^{-1}$ ).

### Growth Respiration

For plants to grow, they require carbohydrates both for their plant-body construction and for

biosynthesis. Here, we define construction cost as the required biomass per actual growth ( $\text{g DM g DM}^{-1}$ ). Thus, the amount of growth respiration of organ  $o$  is  $(RGo - 1.0) \cdot \Delta mass_o$ , where  $RGo$  is the construction cost of organ  $o$ , and  $\Delta mass_o$  is an biomass increment of organ  $o$ . Construction cost can be estimated by combining data on the biochemical composition of organs with knowledge on the biochemical costs of synthesis of all the major compounds, including cellulose, hemicellulose, lignin, protein, lipids, and organic acids (Lambers et al., 1998). Applying this method, Poorter (1994) collected biochemical composition data on various plant species, and then estimated the construction cost of leaves (1.56, mean value of 123 species), stems (1.44, mean value of 38 species), and roots (1.34, mean value of 35 species). Our model employs these parameters with the following two modifications: for grass PFTs, leaves and stems are grouped together as an 'leaf' and thus the two values are averaged (i.e., their collective construction cost is 1.50); the above parameters of Poorter (1994) are estimated mainly from grass species, so we employ 1.68 as the construction cost of a woody stem, because lignin synthesis requires a high expenditure of energy. This value is taken from Penning de Vries (1975), but modified by changing the nitrogen source to  $\text{NO}_3$  as in Poorter (1994).

Individual tree and grass cells have stock resources, which are used for foliation after the dormant phase and after disturbance. In the model, 1.07 of the photosynthetic carbon is consumed while forming a unit amount of stock resource ( $RG_{stockin} = 1.07$ ). This conversion efficiency is taken from the calculation  $1.19 \times (0.400 / 0.444)$ , where 1.19 is the primary photosynthetic product (as glucose) required for producing a unit amount of starch (Tanaka 1983) and 0.400 and 0.444 are carbon mass within a unit mass of glucose and starch, respectively. However, no extra carbon is required when the stock resource is used ( $RG_{stockout} = 1.00$ ), because producing glucose from starch is a simple enzymatic hydrolysis (Penning de Vries et al., 1983).

### Maintenance Respiration

In our simulations, maintenance respiration occurs every day irrespective of phenology phase. The carbohydrates required for maintenance respiration is first charged to the available resource and then the remaining requirements are charged to the stock resource. When the sum of these two resources of carbohydrate is not enough to cover the amount charged, 1% of the biomass of all of the living organs is removed. The removed biomass of sapwood changes to heartwood, while the removed biomass of other organs enters the litter pool. Note that

maintenance respiration does not occur in heartwood or the stock resource.

For a wide variety of plant organs, the maintenance respiration rate is linearly related to the nitrogen content of living tissue (Ryan, 1991). Incorporating this tendency into our model, we calculate the daily maintenance respiration of an organ  $o$  as follows, where constant  $RM$  is the specific respiration rate at 15.0°C (g DM g N<sup>-1</sup> day<sup>-1</sup>),  $PN_o$  is the nitrogen content per biomass of organ  $o$ ,  $tmp$  is air temperature for aboveground organs and soil temperature for underground organs (average soil temperature for soil layers at 0~0.50m depth), and  $qt$  represents the temperature sensibility:

$$RM \times (mass_o \times PN_o) \times \exp\left[\frac{\ln(qt)}{10}(tmp - 15.0)\right]. \quad (24)$$

The temperature sensibility was formulated according to Yokota and Hagihara (1996), as follows:

$$qt = 2.0 \times \exp[-0.009(tmp - 15.0)]. \quad (25)$$

First, we estimated the nitrogen content of the leaves  $PN_f$  for each PFT (Appendix B6) based on a data set from Wright et al. (2004). Then, assuming that the relative proportions of nitrogen in each organ for any particular PFT are linearly correlated, we calculated  $PN_s$  and  $PN_r$  as follows, where the coefficients 0.145 and 0.860 are employed by Friend et al. (1997):

$$PN_s = 0.145 \times PN_f \quad (26)$$

$$PN_r = 0.860 \times PN_f \quad (27)$$

In case of boreal needle-leaved deciduous trees (BoND),  $PN_f$  was taken from an empirical regression equation by Reich et al. (1997) assuming a leaf longevity of three months, because data set of Wright et al. (2004) does not contain a value of BoND. For  $PN_s$  of BoNS, an actual measurement 0.0014 was used (Schulze 1995).

## Turnover

To account for the turnover of organic matter, constant fractions of leaves and fine roots are transformed into litter, while those of sapwood are transformed to heartwood. This turnover occurs every simulation day irrespective of phenology phase. Appendix B6 shows the PFT-specific turnover rates of leaves  $TO_f$ , the data set, which is taken from Wright et al. (2004), does not contain a value for boreal needle-leaved deciduous trees (BoND), so the leaf turnover rate of BoND is assumed to be  $4 \text{ year}^{-1}$  (i.e., a leaf longevity of three months). The turnover rate of fine roots  $TO_r$  is taken from Gill and Jackson (2000). The turnover rate of sapwood  $TO_s$  is assumed to be  $0.05 \text{ year}^{-1}$  for all PFTs, except for TrBE and BoNS. In case of TrBE, a constant fraction of  $dbh$  ( $ALM_5$ ) was assumed to be sapwood, and the remaining fraction was considered heartwood. In case of BoNS, sapwood diameter is assumed to be  $\min[dbh, 0.0188]$  (in m).

## Phenology

Every deciduous PFT in the model has two phenology phases: a growth phase and a dormant phase. Foliation and growth of deciduous PFTs only occurs during the growth phase. The criteria for switching between the two phases, and the procedure of phase change, are described below.

### From Dormant Phase to Growth Phase

Each PFT is classified into the following phenology types, which differ in sub models. A daily computational time step is applied to each sub model.

- Summer green broad-leaved woods (TeBS, BoBS)

One of the phenology control variables is  $gdd5_{Jan}$ , which sums the daily mean air temperature above  $5^\circ\text{C}$  starting on 1 January (for the northern hemisphere) and 1 July (for the southern hemisphere). Trees change from the dormant phase to the growth phase when  $gdd5_{Jan}$  exceeds  $-68 + 638 \times \exp(-0.01 \times i)$ , where  $i$  is the sum of the days for which the mean air temperature is below  $5^\circ\text{C}$ , starting on 1 November (for the northern hemisphere) and 1 May (for the southern hemisphere). Thus, the number of cold days affects the number of days required for phenology change. This sub model is taken from Botta et al. (2000), which is based on the distribution of leaf onset date estimated from remote sensing data. We also assumed that the day of the year ( $doy$ ) of the switch is within the range of 'latitude + 30' to 'latitude + 130' for

the northern hemisphere, and '212 – latitude' to '312 – latitude' for the southern hemisphere.

- Summer green needle-leaved woods (BoNS)

Foliation phase starts when sum of air temperature above 4.1 degree Celsius from January 1 exceeds 65. This sub model is taken from Picard et al. (2005), which is based on the distribution of leaf onset date estimated from remote sensing data.

- Raingreen woody PFT (TrBR)

When 10 day running average of *stat<sub>water</sub>* exceeds 0.0, the dormant phase changes into growth phase.

- Grass PFTs (TeH, TrH)

When optimum leaf area index (*lai<sub>opt</sub>*; formulas described in the section titled 'Growth Procedure of Woody PFTs') exceeds 0 for preceding 7 days, the dormant phase changes into the growth phase.

For the first 14 days (7 days for BoNS, 30 days for TrH) of the growth phase, all of the stock resource is consumed, transformed into available resource at a constant rate. For grass PFTs, this transformation is paused when the optimal leaf area index, *lai<sub>opt</sub>*, is reached.

### **From Growth Phase to Dormant Phase**

At day 60 after the leaf onset date, leaf phenology can change to the dormant phase. At the beginning 14 days of defoliation phase, all leaves are transformed into litter at a constant rate. When plants lost all leaves, if the stock resource does not satisfy the minimum value (100 g individual<sup>-1</sup> for woody PFTs, 50 g m<sup>-2</sup> for grass PFTs), the deficit is supplemented from the litter pool. Each deciduous PFT have distinct condition to change from the growth phase to the dormant phase. When a deciduous PFT does not satisfy the condition, it acts as *de facto* evergreen PFT.

- Temperate summer green broad-leaved woods (TeBS)

The phenology phase is declared dormant if the 10-day running mean of air temperature falls below 9°C or below the 10-year running mean of the coldest month temperature + 5°C.

- Boreal summer green broad-leaved woods (BoBS)  
The phenology phase is declared dormant if soil temperature falls below 2°C. This criteria is from Arora and Boer (2005),
- Boreal summer green needle-leaved woods (BoNS)  
When 10 days of running average of mean air temperature becomes less than 7 °C, leaf defoliation phase occurs, which lasts 14 days. While the defoliation phase, all leaves are transformed into litter at a constant rate.
- Raingreen woody PFT (TrBR)  
The phenology phase is declared dormant when 10 day running average of  $stat_{water}$  falls below 0.0.
- Grass PFTs (TeH, TrH)  
The phenology phase is declared dormant if optimum leaf area index ( $lai_{opt}$ ) falls below 0 for preceding 7 days.

### Growth procedure of woody PFTs

The growth process of woody PFTs consists of four procedures, which differ in computation time steps.

#### Dynamic carbon allocation (daily computation)

During the growth phase, while resource availability ( $mass_{available}$ ) is greater than 0, the following procedures are executed for each individual tree every simulation day.

(1) If the fine root biomass ( $mass_{root}$ ) is less than is required by the functional balance ( $mass_{leaf}/FRratio$ ), the deficit is supplemented from  $mass_{available}$ . Here,  $FRratio$  is the ratio of leaf biomass to fine root biomass satisfying the functional balance.

(2) The stock resource ( $mass_{stock}$ ) is supplemented until it becomes equal to the existing leaf mass ( $mass_{leaf}$ ). However, this step is skipped for the first 30 days of the growing season.



(3) Foliation. There are three constraints on the maximum leaf biomass for each individual: crown surface area ( $max_1$ ), cross-sectional area of sapwood ( $max_2$ ), and available resource ( $max_3$ ). These maximum values (in g DM) are defined as follows:

$$\begin{cases}
 max_1 = (crown_{area} + \pi \times crown_{diameter} \times crown_{depth}) \times LAm_{ax}/SLA & \text{(default, 28)} \\
 max_1 = crown_{area} \times LAm_{ax}/SLA & \text{(for TrBE, 28')} \\
 max_1 = \infty & \text{(for BoNS, 28'')}
 \end{cases}$$
  

$$\begin{cases}
 max_2 = ALM_1 \times \left[ \pi \left( \frac{dbh_{heartwood}}{2} + \frac{dbh_{sapwood}}{2} \right)^2 - \pi \left( \frac{dbh_{heartwood}}{2} \right)^2 \right] / SLA & \text{(Default, 29)} \\
 max_2 = \infty & \text{(for TrBE1~5, TrBR, 29')} \\
 max_2 = 330 \times 50580 dbh^2 & \text{(for BoNS, 29'')}
 \end{cases}$$
  

$$max_3 = mass_{available} / RG_f, \quad (30)$$

where the constant  $SLA$  is the PFT-specific leaf area per unit biomass (Appendix B4).  $SLA$  is primarily taken from data of Wright et al. (2004), but it does not include a value for boreal needle-leaved deciduous trees (BoND); thus, the  $SLA$  value for this type is derived from an empirical regression equation from Reich et al. (1997), assuming a leaf longevity of three months.  $LAm_{ax}$  is the PFT-specific maximum leaf area per unit crown surface area excluding the bottom soffit.  $ALM_1$  is a constant that represents the required area of transport tissue per unit leaf area (Shinozaki et al. 1964a, b). If the current leaf area is less than the  $\min(max_1, max_2, max_3)$ , the deficit is supplemented from  $mass_{available}$ , but maximum daily increment of leaf area is assumed to be 10% of crown surface area.

In case of TrBE1~5, TrBR, and BoNS, negative daily NPP (net primary production) at lowest crown layer suspends new foliation,

(4) Remaining daily computation (5~6) will be omitted under following condition

- During the dormant phase and the first 3 weeks from foliation.
- Annual NPP is less than 10 gDM/tree per year in the previous year.
- Available resource is less than 10.0 gDM/tree.

(5) Reproduction: If total woody biomass is more than 10 kg DM (, which defines minimum tree size for reproduction), 10% of the available resource ( $mass_{available}$ ) is transformed into litter.

(6) The final step of daily growth procedure is trunk growth (except 10g DM/tree, which is for a ‘buffer’ resource for other daily urgent metabolic processes). All of the remaining resource (except 10g DM/tree, which is for a ‘buffer’ resource for other daily metabolic costs) is employed for growth of sapwood biomass ( $mass_{sapwood}$ ). There is no direct allocation to heartwood, which is produced indirectly by slowly converting sapwood. In case of TrBE and BoNS, resource for producing trunk is diminished by multiplying following diminishing factor:

$$1.0 - \frac{mass_{available}}{gpp_{daily}} \times \left( \frac{dbh}{DBH_{limit}} \right)^2, \quad [\text{for TrBE1~4}]$$

$$1.0 - \left( \frac{dbh}{DBH_{limit}} \right), \quad [\text{for BoNS}]$$

where  $gpp_{month}$  is monthly GPP for each individual tree and  $DBH_{limit}$  is the PFT-specific maximum  $dbh$  (m). This equation assumes that stem growth efficiency becomes lower when  $dbh$  approaches to their maximum limits. The reduced resource is consumed by maintenance respiration.

Increments of sapwood biomass are accompanied by growth in sapwood diameter ( $dbh_{sapwood}$ ) and trunk height ( $height$ ). These increments ( $\Delta dbh_{sapwood}$  and  $\Delta height$ ) must satisfy the

following two trunk mechanics.

(A) Trunk mechanics 1: a relationship between trunk biomass and trunk geometry. Trunk biomass, a function of tree height (*height*) and trunk diameter, is calculated as follows, where  $ALM_3$  is dry mass per unit timber volume (in g DM m<sup>-3</sup>):

$$mass_{trunk} = ALM_3 \times \pi \left( \frac{dbh}{2} \right)^2 \times height \quad [\text{Default}]$$

$$mass_{trunk} = \pi \times \left( \frac{dbh}{2} \right)^2 \times height \times ALM_3 \times [-0.0108 \times \ln(mass_{trunk}) + 0.5941] / 0.7$$

[for TrBE1~4]

$$mass_{trunk} = 2.516 \times ALM_3^{1.036} \times dbh^{2.179} \quad [\text{for TrBE5, TrBR}]$$

$$mass_{trunk} = \min \left[ 1.5(367dbh^2 \times 10^4 - 11300), 190(100dbh)^{1.81} + 42.8(100dbh)^{1.79} + 171(100dbh)^{1.67} \right]$$

[for BoNS]

The value of  $ALM_3$  for TrBE and BoNS were obtained from Huth and Ditzer (2000) and Schulze et al. (1995), respectively. For other broad-leaved PFTs and evergreen needle-leaved PFTs were calculated by averaging 46 broad-leaved woody species and 24 needle-leaved woody species from Japan; the data were obtained from a table in *The Handbook of Wood Industries* (FFPRI, 1982). It should be noted that the table excluded pioneer woody species, which typically produce low-density timber, and that the SEIB–DGVM assumes that the trunk has a cylindrical shape that extends to the top of the crown (Fig. 1). Thus, the estimated trunk biomass (from default equation) should exceed the actual biomass for the same trunk diameter at bottom with tapered trunk shape; however, because the model includes branches and coarse roots as trunk biomass, this simplification might be justified.

(B) Trunk mechanics 2: a relationship between trunk diameter and maximum tree height for that diameter, calculated as follows, where the parameters  $HGTs$  and  $HGTmax$  are the initial growth slope and the maximum tree height for an infinite trunk diameter,

respectively:

$$height \leq \left[ \frac{1}{HGTs \times (dbh_{sapwood} + dbh_{heartwood})} + \frac{1}{HGTmax} \right]^{-1}. \quad (32)$$

In the model, the crowns of different trees cannot occupy the same space. Thus, when the crowns of neighboring trees interfere with tree height, only the trunk diameter expands.

### Expansion of a cross-section area of the crown (daily computation)

Crown expansion is calculated as follows, where the constant  $ALM_2$  is assumed to be 100.0 for every needle-leaved PFT and 200.0 for every broad-leaved PFT:

$$crown_{area} \leq ALM_2 \times (dbh_{sapwood} + dbh_{heartwood})^{1.6} \quad [\text{Default}]$$

$$\left\{ \begin{array}{ll} crown_{diameter} = (50 - 125 \times dbh) \times dbh & [\text{for TrBE1~4 } (dbh < 0.2)] \\ crown_{diameter} = 25 \times dbh & [\text{for TrBE1~4 } (dbh \geq 0.2)] \end{array} \right.$$

$$crown_{diameter} = 0.64 \times height \quad [\text{for TrBE5, TrBR}]$$

$$crown_{area} \leq 80 \times (dbh_{sapwood} + dbh_{heartwood}) \quad [\text{for BoNs}]$$

These equations for default, BoNS, and TrBE are based on inversion of Reineke's rule (Zeide, 2001), forest inventory data (Yabuki personal commu.), and Köhler and Huth (1998), respectively. The crown size has additional two constraints: it can neither exceed its

maximum limit ( $CD_{max}$ ) nor expand into neighboring crowns.

### **Crown depth adjustment (annual computation)**

On the last day of each year, the height of the lowest branch increases as a result of purging crown disks, or self pruning of branches, at the bottom of the crown layer. This procedure is conducted even if the tree is in the dormancy phase. A maximum of 10 crown disks can be pruned at one time, each at a depth of 10 cm. Consequently, and because elongation of the lowest branch is linked to crown pruning, the maximum increase in height of the lowest branch is  $100 \text{ cm year}^{-1}$ .

To determine the number of crown disks to purge, we first calculate the annual GPP for each crown disk. Then, the mean of the GPP for each of the 10 crown groups (1–10 successive disks from the crown bottom) for each tree is calculated. These values are divided by the GPP of the top crown disk of each tree, and then fraction is used to select disks for purging. Those with fraction less than  $ALM_4$  are selected for pruning; of these, the group that includes the largest number of crown disks is pruned. It should be noted that pruning is also constrained by  $crown_{depth}$ , which must always exceed 10 (i.e.,  $>100 \text{ cm}$ ) and that once a crown disk is pruned, it cannot reestablish (i.e., the height of the lowest branch cannot decrease).

In case of TrBE1~5 and TrBR, crown depth (m) is proportional to tree height. The ratio of crown depth to tree height ( $ALM_6$ ) was derived from Huth (1998) for TrBE1~4. While  $ALM_6$  of TrBE5 and TrBR are assumptions. In case of BoNS, crown depth (m) is assumed to be  $\min[10, height]$ .

In case of BoNS, crown vertical depth was assumed to be 10 cm. For trees less than 10m tall, crown was assumed to start from 1.3m aboveground height.

### **Crown horizontal location adjustment (annual computation)**

On the last day of each year, the crown center moves horizontally toward the most open direction. This crown movement represents the fact that trees extend their branches into open and bright spaces. Without introducing this plasticity, interference among crowns severely limits the number of tall trees, because crowns of different trees cannot occupy the same space in the SEIB–DGVM. The maximum speed of crown movement is assumed to be 20 cm

year<sup>-1</sup>, and the maximum distance of the movement is equal to half of the crown radius (i.e., the distance between the bole and crown centers is less than half of the crown radius).

### Growth Process of Grass PFTs (Daily Computation)

During the growth phase, while resource availability ( $gmass_{available}$ ) is greater than 0, the following procedures are executed every simulation day.

(1) If root biomass ( $gmass_{root}$ ) is less than that required by the functional balance ( $gmass_{leaf}/FRratio$ ), the deficit is supplemented.

(2) The stock resource ( $gmass_{stock}$ ) is supplemented until it becomes 1.3 (a tuning parameter) times to the existing leaf biomass ( $gmass_{leaf}$ ). This step is omitted for the first 30 days of the growing season.

(3) The leaf biomass ( $gmass_{leaf}$ ) is supplemented until the leaf area index of the PFT ( $lai_g$ ) reaches a weekly running mean equal to the optimal leaf area index  $lai_{opt}$ , which maximizes daily net primary production,  $gpp_g - cost \times lai_g/SLA$  (derived from equations 19 and 34). This variable is calculated as follows, where  $cost$  is the cost of maintaining leaves per unit leaf mass per day (see equation 34 for the definition):

$$lai_{opt} = \frac{\ln par_{grass} - \ln \left\{ \frac{p_{sat}}{lue} \left[ \left( 1 - \frac{cost / SLA}{0.09093 \times dlen \times p_{sat}} \right)^{-2} - 1 \right] \right\}}{eK}. \quad (36)$$

(4) All remaining resource ( $gmass_{available}$ ) is used for reproduction, and then transformed into litter. This step is omitted for the first 30 days of the growing season and when the stock resource is less than 100 g DM m<sup>-2</sup>.

### Mortality (except death by fire and gap formation)

Mortality is explicitly modeled only for woody PFTs. On the last day of each simulation year,

the overall death rate is calculated for each individual tree as a sum of mortality components, which consist of background mortality, heat stress, and bioclimatic limit. These components are basically derived from the LPJ–DGVM (Sitch et al., 2003). It is also assumed that newly established trees do not die in their first 2 years. If annual NPP of the previous year is negative, 10 times larger background mortality will be applied for African woody PFTs, same background mortality will be applied for BoNS, while other woody PFTs will immediately die. A tree also dies (except for BoNS). A tree also dies if the trunk diameter is more than 1.0 m.

Background mortality is related to growth efficiency, which seems to be a sensitive indicator of resistance to environmental stress (Warning, 1983). Although there is no standard formula for background mortality, the model assumes the following, where  $anpp$  is the annual sum of net primary production (g DM),  $la_{mean}$  is the mean leaf area of the previous year ( $m^2$ ), and  $M_1$  ( $\leq 1.0$ ) and  $M_2$  ( $\geq 1.0$ ) are PFT-specific mortality coefficients:

$$\frac{M_1}{M_2 \frac{anpp}{la_{mean}}} \quad [\text{Default}]$$

In case of TrBE1~4, background mortality is modeled as a function of the annual incremental increase of  $dbh$  ( $\Delta dbh$  in  $m\ yr^{-1}$ ), which was regressed from Table 3 of Huth and Ditzer (2000;  $r^2 = 0.98$ ) as follows:

$$\max[0.0178 \times \exp(-242.57 \times \Delta dbh), 0.0032] \quad [\text{for TrBE}]$$

This carbon balance mortality is multiplied by 8.0 for TrBE3. According to Huth and Ditzer (2000), I distinguished five canopy layers (0~1.3 m, 1.3~15 m, 15~25 m, 25~36 m, and >36 m) to determine whether specific overcrowded-mortality-rate will be applied. For each tree, sum of crown area overlapped by other crowns within the same canopy layer was computed, and if it exceeds crown area of the subjected tree, the higher background mortality 0.04 (for TrBE1, TrBE2, and TrBE4) and 0.08 (for TrBE3) are applied instead of the above mortality.

Mortality by bioclimatic limit restricts the climate range in which each PFT can survive. If the 20-year mean of the coldest month temperature is less than the PFT-specific limit  $TC_{min}$ , all

individuals of the PFT die immediately. Boreal needle-leaved summergreen trees (BoNS) have an additional bioclimatic limit: if the 20-year mean of (warmest–coldest monthly air temperature) is less than 43°C, all trees of the PFT die. Biomass of dead trees is forming new litter.

#### Disturbance by Fire (default, daily computation)

We employed the global fire model of Thonicke et al. (2001), which was developed for the LPJ–DGVM. On the last day of each simulation year, if the fuel load (litter + aboveground biomass) satisfies the minimum threshold (200 g C m<sup>-2</sup>), the probability of fire is calculated as a function of moisture fraction in the fuel,  $\theta$ , as follows:

$$s \times \exp\left(\frac{s-1}{0.45(s-1)^3 + 2.83(s-1)^2 + 2.96(s-1) + 1.04}\right), \quad (39)$$

, where variable  $s$  is

$$s = \sum_{day=1}^{365} \exp\left[-\pi\left(\frac{\theta}{m_e}\right)^2\right] / 365. \quad (40)$$

Variable  $m_e$  in equation 40, which takes into consideration the difference in fire extinction efficiency between woody and grass PFTs, is defined as  $0.3 \times (\text{aboveground biomass of trees}/\text{total aboveground biomass}) + 0.2 \times (\text{leaf biomass of grass}/\text{total aboveground biomass})$ . Here, moisture fraction of the fuel,  $\theta$ , is assumed half of the moisture fraction in the top soil layer (0-50cm depth).

The model also assumes that fire cannot occur in two consecutive years.

The fraction of individuals killed in a fire depends on PFT fire resistance ( $M_3$ , Appendix B5). During a fire, all leaf biomass of grass, all leaf biomass of dead and surviving trees, half of the trunk biomass of dead trees, and half of the litter pool are released into the atmosphere as CO<sub>2</sub>, while the remaining biomass of dead trees is transformed into litter. In response to fire,



the phenology phase of all grass PFTs changes to dormant (they reenter the growth phase as described previously in the section titled ‘Phenology’). If the stock resource of grass PFTs ( $gmass_{stock}$ ) does not satisfy the minimum value ( $50 \text{ g DM m}^{-2}$ ) after fire, the deficit is supplemented from litter.

#### Disturbance by Fire (for African continent, daily computation)

Wildfire frequently occurs in African savannas, leading to tree and grass death and litter consumption. For simulations of the African continent, we introduced a fire sub-model of aDGVM (Scheiter 2009) with some simplifications. This sub-model is a semi-empirical model that is based largely on data from southern African studies of savanna.

The litter pool is composed of three pools: standing dead mass of tree leaves, standing dead mass of grass, and lying dead mass. The litter flux from tree leaves was first added to the “standing dead mass of tree leaves,” and the litter flux from grass aboveground biomass was first added to the “standing dead mass of grass.” Both standing dead pools convert into “lying dead mass” at a rate of 0.075% per day. Beside reclassification of litter pools with different combustibility, all litter pools decompose with the same function of soil moisture and air temperature (Sato 2007).

For each grass cell, the potential energy intensity on the fire line ( $ifire$  in  $\text{J s}^{-1}\text{m}^{-1}$ ) is estimated as a function of the fuel load in the grass cell ( $fuel$  in  $\text{gDM m}^{-2}$ ), the fraction of fuel moisture ( $\theta$ ), and the wind speed ( $wind$  in  $\text{m s}^{-1}$ ):

$$ifire(fuel, \theta, wind) = 16890 \times \left( fuel \frac{fuel}{fuel + 119.7} \right) \times \left( \frac{301 \times \arctan(wind)}{2.6 \times 10^3 \times \theta + 1.61 \times 10^5 (1 - \theta)} \right)$$

Here, 16890 is the typical heat yield when fuel is consumed (in  $\text{J g}^{-1}$ ); 119.7 and 301 are coefficients; and  $2.6 \times 10^3$  and  $1.61 \times 10^5$  are the preignition heat of moisture and fuel (in  $\text{J g}^{-1}$ ), respectively. The first parenthetical term is the weight of fuel consumed (in  $\text{gDM m}^{-2}$ ) and the second parenthetical term is the rate of fire spread (in  $\text{m s}^{-1}$ ). These coefficients and fuel preignition heat are estimated from field observations during data collection campaigns conducted in grassland and savanna in South Africa.

For estimating the *fuel* and  $\theta$ , fuel load was divided into living (moist) fuel *fuel<sub>living</sub>* and dead (dry) fuel *fuel<sub>dead</sub>*.

$$fuel = fuel_{living} + fuel_{dead}$$

Living fuel, *fuel<sub>living</sub>*, is the sum of the aboveground grass biomass, *gmass<sub>leaf</sub>*, and one-half of the standing dead mass of grass, *fuel<sub>standing</sub><sup>grass</sup>*. Dead fuel, *fuel<sub>dead</sub>*, is the sum of lying dead mass, *fuel<sub>lying</sub>*, and one-half of the grass standing dead mass, *fuel<sub>standing</sub><sup>grass</sup>*.

$$fuel_{living} = gmass_{leaf} + 0.5 \times fuel_{standing}^{grass}$$

$$fuel_{dead} = fuel_{lying} + 0.5 \times fuel_{standing}^{grass}$$

The moisture content of living fuel is assumed to be equal to the relative air humidity, *rh*. The moisture content of dead fuel is assumed to be 0%, because it quickly decreases with an exponential function (Higgins 2000). Hence, average fuel moisture,  $\theta$ , is given as follows:

$$\theta = rh \times \frac{fuel_{living}}{fuel_{living} + fuel_{dead}}$$

For the occurrence of a fire, stand average of the potential fire intensity, *ifire*, must exceed a minimum intensity of 300 kJ s<sup>-1</sup>m<sup>-1</sup> (van Wilgen 1997). When this condition is satisfied, the probability of fire in a day is 0.0015 (Scheiter and Higgins, 2009). This probability is reduced by 80% and 100%, if the fraction of the tree canopy coverage of the stand (0.0–1.0) is 0.40–0.65 and 0.65, respectively (Archibald et al., 2009). This reduction imitates a phenomenon where the fuel load in tree stands with high canopy coverage is shaded and dries out more slowly. The fire sub-model is actuated on every simulation day.

Fire consumes all the aboveground biomass of grass, standing dead mass of grass and tree leaves, lying dead mass, and half of trunk litter. Fire changes grass phenology to dormant. Fire also causes tree mortality. Following (Higgins 2000), tree mortality due to wildfire is an empirically derived function of tree height, *height* (m), and fire intensity, *ifire*, of the tree standing grass cell.

$$mort_{fire}(height, ifire) = \frac{\exp[d_1 - d_2 \ln(height) + d_3 \sqrt{ifire}]}{1 + \exp[d_1 - d_2 \ln(height) + d_3 \sqrt{ifire}]}$$

where the coefficients  $d_1$ ,  $d_2$ , and  $d_3$  are 4.3, 5.003, and 0.004408, respectively.

#### Disturbance by Gap formation

When biome type is tropical rain forest, following computation is conducted. When a large tree (*height* > 25 m) dies, gap formation (healthy trees are knocked over by falling trees) occurs at a probability of 0.20. When this occurs, trees within the gap will be killed at tree height-specific probabilities: 0.3 for trees of 1.3~15 m height, 0.6 for trees of 15~25 m height, 0.8 for trees of 25~36 m height, and 0.4 for trees >36 m height. These formulations are based on those of FORMIX3 (Huth and Ditzer 2000). Hence, to match the 20 × 20-m square gap size in FORMIX3, a circular-shaped gap of 11.3-m radius was assumed to appear in a random location within the virtual forest.

#### Soil Respiration

The decomposition of litter and soil organic carbon is calculated for each simulation day. The SEIB-DGVM employs the soil respiration module of the DEMETER-1 (Foley, 1995) with some simplifications. The mean turnover rate of litter at 20°C and ample soil moisture is assumed to be 3/10 year<sup>-1</sup>. 70% of the decomposed litter carbon is released into the atmosphere as CO<sub>2</sub>, and the remaining 30% becomes soil organic carbon. The partitioning coefficients for soil organic carbon flowing into the fast and slow decomposition pools are 0.985 and 0.015, respectively. According to Foley (1995), the mean turnover rates for the fast and slow soil organic carbon ( $TO_{fast}$ ,  $TO_{slow}$ ) at 20°C and ample soil moisture are 1/15 year<sup>-1</sup> and 1/750 year<sup>-1</sup>, respectively.

Actual daily turnover rates ( $k_n \text{ day}^{-1}$ ), which are adjusted according to soil environment, are approximated as follows, where  $g$  and  $f$  are functions of the monthly mean soil temperature (averaged for 0~0.50m depth) and moisture, respectively:

$$k_n = \left[ \frac{TO_n}{365} \times g(tmp_{soil}) \times f(pool_{w(l)}) \right] \quad (42)$$

These functions are defined as follows:

$$g(tmp_{soil}) = \exp \left( 308.56 \times \left( \frac{1}{66.02} - \frac{1}{tmp_{soil} + 46.02} \right) \right) \quad (43)$$

$$f(pool_{w(l)}) = 0.25 + 0.75 \left( \frac{pool_{w(l)}}{W_{fi} \times Depth_{(l)}} \right) \quad (44)$$

In Foley (1995), the temperature effect  $g(tmp_{soil})$  is an exponential function. However, this underestimates the soil turnover rate for cold regions, and thus we employ the function of Lloyd and Taylor (1994). All decomposed soil organic carbon is released into the atmosphere as  $CO_2$ .

## Appendix A

### A1. Atmospheric environments (computed daily)

Atmospheric conditions were calculated daily based on input climate data. Air pressure ( $ap$  in hPa) was approximated by site altitude ( $ALT$  in m) and air temperature ( $tmp_{air}$  in °C):

$$ap = 1013.25 \times \exp\left(\frac{-0.2838472 \times ALT}{8.3144(tmp_{air} + 273.15)}\right), \quad (A1)$$

where the multiplier 1013.25 is the control air pressure (in hPa) at sea level at 15°C, and the multiplier 8.3144 is the universal gas constant (in J mol<sup>-1</sup> K<sup>-1</sup>). Actual vapor pressure ( $vp$  in hPa) was a function of air pressure  $ap$  and humidity  $humid$  (g g<sup>-1</sup>):

$$vp = \frac{ap \times humid}{0.622 + 0.378 \times humid}, \quad (A2)$$

The saturated vapor pressure  $vp_{sat}$  (hPa) was given by Tetens' equation:

$$vp_{sat} = 6.1078 \times 10^{\frac{7.5tmp_{air}}{237.3+tmp_{air}}} \quad (tmp_{air} > 0.0) \quad (A3)$$

$$vp_{sat} = 6.1078 \times 10^{\frac{9.5tmp_{air}}{265.3+tmp_{air}}} \quad (tmp_{air} \leq 0.0). \quad (A4)$$

The vapor pressure deficit  $vpd$  (hPa) is the difference between saturated and actual vapor pressures:

$$vpd = vp_{sat} - vp. \quad (A5)$$

The slope of saturated vapor pressure  $slope_{vps}$  (hPa °C<sup>-1</sup>) is:

$$slope_{vps} = \frac{6.1078 \times (2500 - 2.4tmp_{air})}{0.4615(tmp_{air} + 273.15)^2} \times 10^{\frac{7.5tmp_{air}}{237.3 + tmp_{air}}} \quad (tmp_{air} > 0.0) \quad (A6)$$

$$slope_{vps} = \frac{6.1078 \times 2834.0}{0.4615(tmp_{air} + 273.15)^2} \times 10^{\frac{9.5tmp_{air}}{265.3 + tmp_{air}}} \quad (tmp_{air} \leq 0.0). \quad (A7)$$

The density of air  $dnsa$  (kg m<sup>-3</sup>) is:

$$dnsa = 1.293 \frac{ZAT}{tmp_{air} + ZAT} \times \frac{ap}{1013.25} \times \left( 1 - 0.378 \frac{vp}{ap} \right). \quad (A8)$$

## A2. Solar radiation (computed daily)

Angular solar elevation above the horizontal at midday ( $sl_{hgt}$ ) was calculated by the following equations:

$$\sin(sl_{hgt}) = \sin(LAT) \times \sin(sl_{dec}) + \cos(LAT) \times \cos(sl_{dec}), \quad (A9)$$

where  $LAT$  is the site latitude ( $-90 \leq LAT \leq 90$  in degree) and  $sl_{dec}$  is the solar declination of the earth's orbit in degrees.  $sl_{dec}$  has a maximum value of 23.4 on the summer solstice, and a minimum value of -23.4 on the winter solstice, and a value of 0 on equinox days; thus, it can be approximated by the following equation:

$$sl_{dec} = 23.4 \sin(360 \times (doy - 81) / 365), \quad (A10)$$

where *doy* is the days of the year (1–365, ignoring leap years). Using  $sl_{dec}$ , the hourly angle of the sun from sunrise to midday can be calculated as  $\arccos(-\tan(LAT) \times \tan(sl_{dec}))$ ; thus, the day length in hours (*dlen*) will be:

$$dlen = 2 [\arccos(-\tan(LAT) \times \tan(sl_{dec})) / 15]. \quad (A11)$$

Shortwave radiation at the top of the atmosphere at midday ( $rad_{intact}$  in  $\text{W m}^{-2}$ ) is a function of  $sl_{hgt}$ :

$$rad_{intact} = 1367 \times \sin(sl_{hgt}) \times (ESD_{mean}/ESD)^2, \quad (A12)$$

where the multiplier 1367 is a solar constant (in  $\text{W m}^{-2}$ ),  $ESD$  is the distance between the sun and the earth (in km), and  $ESD_{mean}$  represents the annual mean  $ESD$  ( $=1.46 \cdot 10^8$  km).  $(ESD_{mean}/ESD)^2$  can be approximated by:

$$(ESD_{mean}/ESD)^2 = 1.000111 + 0.034221 \cos(x) + 0.00128 \sin(x) + 0.000719 \cos(2x) + 0.000077 \sin(2x), \quad (A13)$$

where  $x$  is the seasonal angle of the earth's orbit ( $x = 360 \times doy / 365$ ). In the troposphere, the incident solar radiation  $rad_{intact}$  ( $\text{W m}^{-2}$ ) is attenuated by clouds and airborne particles. This effect has been empirically formulated as a function of cloud cover ( $0.0 \leq cloud \leq 0.8$ ) by Itoh (personal communication) based on NCEP/NCAR data, as follows:

$$rad = rad_{intact} \times (0.8964 - 0.5392 \text{ cloud}), \quad (A14)$$

where  $rad$  is the amount of solar radiation that reaches to the biosphere (in  $\text{W m}^{-2}$ ).

In addition to this attenuation effect on irradiance, scattering in the atmosphere optically alters the ratio between direct and diffuse radiation:

$$rad_{diffuse} = rad \times [ 0.958 - 0.982 (rad/rad_{intact}) ] \quad (A15)$$

$$rad_{direct} = rad - rad_{diffuse}, \quad (A16)$$

where  $rad_{diffuse}$  and  $rad_{direct}$  are diffuse radiation and direct radiation within  $rad$ , respectively. Diffuse and direct radiation differ in their fractional content of photosynthetically active radiation (PAR: 400–700 nm) in the total spectrum; diffuse radiation contains 57%, while direct radiation contains 43%. Thus, photosynthetic photon flux density of PAR is given by the following:

$$par_{diffuse} = 4.2 \times 0.57 \times rad_{diffuse} \quad (A17)$$

$$par_{direct} = 4.6 \times 0.43 \times rad_{direct} \quad (A18)$$

$$par = par_{diffuse} + par_{direct} \quad (A19)$$

where  $par$  is photosynthetically active radiation at midday (in  $\mu\text{mol photon m}^{-2} \text{ s}^{-1}$ ), and  $par_{diffuse}$  and  $par_{direct}$  are the diffused and direct radiation components of  $par$ . The multipliers 4.2 and 4.6 are for unit conversion from  $[\text{W m}^{-2}]$  to  $[\mu\text{mol photons m}^{-2} \text{ s}^{-1}]$  for diffuse and direct radiation, respectively (Larcher, 1995).

### A3. Net Radiation (Computed Daily)

To estimate the transpiration rate of leaves and the evaporation rate of soil, the net radiation at vegetation ( $radnet_{veg}$  in  $\text{W m}^{-2}$ ) and at the soil surface ( $radnet_{soil}$  in  $\text{W m}^{-2}$ ) were calculated as:



$$radnet_{veg} = [rad \times (1 - albedo_{veg}) + radnet_{long}] \times (1 - ir) \quad (A20)$$

$$radnet_{soil} = [rad \times (1 - albedo_{soil}) + radnet_{long}] \times ir, \quad (A21)$$

where  $ir$  is the shortwave interception by leaves:

$$ir = \exp\left(\sum_p^{pft} (-eK_p \times lai_p)\right) \quad (A22)$$

and  $albedo_{veg}$  and  $albedo_{soil}$  are the albedo of vegetation and the soil surface, respectively;  $albedo_{veg}$  was assumed to be 0.15 for forest biome and 0.24 for other biome (Jones 1992). On the other hand,  $albedo_{soil}$  was assumed be a function of soil albedo ( $ALBEDO$ ) and the amount of snow on the ground:

$$albedo_{soil} = ALBEDO + (0.7 - ALBEDO)/[1 + \exp(-0.05(pool_{snow} - 70.0))]. \quad (A23)$$

The  $radnet_{long}$  is net long-wave radiation, which is estimated by the following empirical formula:

$$radnet_{long} = 5.67 \times 10^{-8} \times (tmp_{air} + 273.15)^4 \times (1 - 0.65 \text{ cloud}) \times [0.39 + 0.058/(vp + 1.0)], \quad (A24)$$

where the constant  $5.67 \times 10^{-8}$  is Stefan–Boltzmann's constant (in  $W \text{ m}^{-2} \text{ K}^{-4}$ ).

#### A4. Parameters of Photosynthesis and Stomatal Conductance (Computed Daily)

Appendix B7 shows the definition of PFT-specific photosynthesis parameters. To estimate photosynthesis and stomatal conductance, daily averages of photosynthetic rates ( $p_{ave}$  in  $\mu\text{mol CO}_2 \text{ m}^{-2} \text{ s}^{-1}$ ) was calculated for each PFT of each scale of one to ten relative PAR intensity

(10%, 20%, ..., 100% relative PAR intensity to the top of the forest canopy of the day), using equation (15):

$$p_{ave} = \frac{p_{sat} \times lue \times x}{p_{sat} + lue \times x}, \quad (A25)$$

where  $p_{sat}$  is single-leaf photosynthetic rate under light saturation (in  $\mu\text{mol CO}_2 \text{ m}^{-2} \text{ s}^{-1}$ ).  $x$  is the daily average of PAR receiving for grass layer (for grass PFTs) or for crown disk of trees (for woody PFTs) (in  $\mu\text{mol photon m}^{-2} \text{ s}^{-1}$ ).  $lue$  is the light-use efficiency of photosynthesis (in  $\text{mol CO}_2 \text{ mol photon}^{-1}$ ), which is formulated to conform to the data in Osmond et al. (1980) as follows:

$$lue = LUE \times \frac{52 - tmp_{air}}{3.5 + 0.75(52 - tmp_{air})} \times \frac{co2_{cell}}{90 + 0.6 \times co2_{cell}} \quad (\text{for } C_3 \text{ PFTs}) \quad (A26)$$

$$lue = LUE \quad (\text{for } C_4 \text{ PFTs}), \quad (A27)$$

where  $LUE$  is the potential maximum value, and  $co2_{cell}$  is the intercellular  $\text{CO}_2$  concentration (in  $\mu\text{mol mol}^{-1}$ ). The single-leaf photosynthetic rate,  $p_{sat}$ , under light saturation (in  $\mu\text{mol CO}_2 \text{ m}^{-2} \text{ s}^{-1}$ ), is calculated by multiplying its potential maximum of photosynthetic rate ( $PMAX$ ) by the coefficients of temperature,  $\text{CO}_2$  level, and soil water effects ( $ce_{tmp}$ ,  $ce_{co2}$ , and  $ce_{water}$ , respectively):

$$p_{sat} = PMAX \times ce_{tmp} \times ce_{co2} \times ce_{water}. \quad (A28)$$

$ce_{tmp}$ , the temperature-dependent function of  $p_{sat}$ , is a bell-shaped curve that reaches the maximum (1.0) at the optimum temperature and tapers off in warmer or cooler temperatures (Raich et al., 1991):

$$ce_{tmp} = \frac{(tmp_{air} - T_{max})(tmp_{air} - T_{min})}{(tmp_{air} - T_{max})(tmp_{air} - T_{min}) - (tmp_{air} - t_{opt})^2}, \quad (A29)$$

where  $T_{max}$ ,  $T_{min}$ , and  $t_{opt}$  are the PFT-specific maximum, minimum, and optimum temperature for photosynthesis, respectively (in °C).  $t_{opt}$  increases with the intercellular CO<sub>2</sub> concentration because of photorespiration:

$$t_{opt} = T_{opt0} + 0.01 \text{ } co2_{cell} \quad (A30)$$

where  $T_{opt0}$  is the minimum value of  $t_{opt}$  at a very low  $co2_{cell}$ . For grass PFTs,  $t_{opt}$  is assumed to be a 20-year running mean of air temperature in the growth phase (maximum range 10°C–30°C for TeH and 20°C–40°C for TrH), because grass PFTs includes a varieties of species adapted to a wide range of climatic zones.

The  $ce_{co2}$ , the CO<sub>2</sub>-dependent function of  $p_{sat}$ , is expressed by a Michaelis-type function:

$$ce_{co2} = 0.30 + 0.70 \times \frac{co2_{cell} - co2_{cmp}}{KM + co2_{cell}} \quad (\text{for } C_3 \text{ PFTs}) \quad (A31)$$

$$ce_{co2} = 0.50 + 0.50 \times \frac{co2_{cell} - co2_{cmp}}{KM + co2_{cell}} \quad (\text{for } C_4 \text{ PFTs}), \quad (A32)$$

where  $KM$  is the coefficient of CO<sub>2</sub> concentration sensitivity;  $co2_{cmp}$  is the CO<sub>2</sub> compensation point, which is adjusted by temperature for  $C_3$  species (Brooks and Farquhar, 1985).

$$co2_{cmp} = CO2cmp [1 + 0.0451(tmp_{air} - 20) + 0.000347(tmp_{air} - 20)^2] \quad (\text{for } C_3 \text{ PFTs}) \quad (A33)$$

$$co2_{cmp} = CO2cmp \quad (\text{for } C_4 \text{ PFTs}), \quad (A35)$$

where  $CO2_{cmp}$  is the control value of  $co2_{cmp}$  at 20°C;  $ce_{water}$ , the water availability effect coefficient of  $p_{sat}$ , is calculated as follows:

$$ce_{water} = 2 \times stat_{water} - (stat_{water})^2. \quad (A35)$$

This function reconstructs a generally observed phenomenon in which the ratio of actual evaporation to potential evaporation has high sensitivity to soil water content near the wilting point, while sensitivity is reduced near field capacity (Dunne and Leopold 1978)

The mean daytime crown stomatal conductance of H<sub>2</sub>O  $gs_{ave}$  (mol H<sub>2</sub>O m<sup>-2</sup> s<sup>-1</sup>), is obtained by equation 20:

$$gs_{ave} = GS_{b1} + \frac{GS_{b2} \times p_{ave}}{(co2_{atm} - co2_{cmp})(1 + vpd / GS_{b3})}, \quad (A36)$$

where  $GS_{b1}$ ,  $GS_{b2}$ , and  $GS_{b3}$  are PFT-specific parameters;  $gs_{ave}$  affects the intercellular CO<sub>2</sub> concentration ( $co2_{cell}$  in  $\mu\text{mol mol}^{-1}$ ) following Leuning (1990):

$$co2_{cell} = co2_{atm} - \frac{p_{ave}}{gs_{ave} / 1.56}, \quad (A37)$$

where 1.56 is a factor to convert  $gs$  into CO<sub>2</sub> conductance. Using equations A25 through A37, we calculated  $p_{ave}$ ,  $lue$ , and  $gs_{ave}$  of each PFT every simulation day.

#### A6. Evapotranspiration (Computed daily)

The potential evaporation ( $ev_{pm}$ ) and transpiration ( $tr_{pm}$ ) are estimated by the Penman–Monteith method (Monteith and Unsworth, 1990), assuming an abundant water supply:

$$ev_{pm} = \frac{dlen \times 0.5 \times slope_{vps} \times radnet_{soil} + 24 \times 1012 \times dnsa \times vpd \times c_{aero}}{lh \{ slope_{vps} + 0.667(1.0 + c_{aero} / c_{soil}) \}}, \quad (A44)$$

$$tr_{pm} = \frac{dlen \times 0.5 \times slope_{vps} \times radnet_{veg} + dlen \times 1012 \times dnsa \times vpd \times c_{aero}}{lh \{ slope_{vps} + 0.667(1.0 + c_{aero} / c_{leaf}) \}} - ic, \quad (A45)$$

where  $dlen$  is day length (in hour),  $slope_{vps}$  is saturated vapor pressure (in hPa °C<sup>-1</sup>),  $dnsa$  is density of air (in kg m<sup>-3</sup>),  $vpd$  is vapor pressure deficit (in hPa), and  $ic$  is intercepted precipitation (in mm day<sup>-1</sup>).  $0.5 \times radnet_{veg}$  and  $0.5 \times radnet_{soil}$  are the daytime average of net radiation on leaves and soil surface when daily change of radiation was approximated by sin<sup>2</sup>. The constant 24 is the day length (in hour day<sup>-1</sup>), 1012 is the specific heat of air (in J kg<sup>-1</sup> K<sup>-1</sup>), and 0.667 is the psychrometer constant (in hPa K<sup>-1</sup>).  $lh$  is the latent heat of water (in Wh kg<sup>-1</sup> H<sub>2</sub>O).

$$lh = \frac{1000 \times [2259 - 4.2 \times (100 - tmp_{air})]}{3600},$$

where 2259 and 4.2 are vaporization heat and water specific heart (J g<sup>-1</sup> H<sub>2</sub>O), and 3600 is unit converter from second to hour.

$c_{aero}$ ,  $c_{soil}$ , and  $c_{leaf}$  are aerodynamic conductance, soil surface conductance, and canopy conductance, respectively.

$$c_{aero} = \frac{1.0 + 0.537 \times wind}{250.1}. \quad (A46)$$

This equation was delivered by substituting empirical formulation of Penman (1948) into equation A44.  $c_{soil}$ , soil surface conductance, is in proportion to the fraction of soil layer 1 that is saturated with water:

$$c_{soil} = 0.0015 \times \min \left[ \left( \frac{\sum_{i=1,5} pool_{w(i)}}{Wfi \times Depth \times 5} \right)^2, 1 \right], \quad (A47)$$

where the multiplier 0.0015 (this is just only a tuning parameters) is water-saturation conductance, which is a tuning parameter Finally,  $c_{leaf}$  is

$$c_{leaf} = 0.0224 \times ccon, \quad (A48)$$

where  $ccon$  is mean daytime stomatal conductance of the simulated forest (in  $\text{mol H}_2\text{O m}^{-2} \text{s}^{-1}$ ), and the multiplier 0.0224 is the unit converter from  $[\text{mol H}_2\text{O m}^{-2} \text{s}^{-1}]$  to  $[\text{m}^3 \text{H}_2\text{O m}^{-2} \text{s}^{-1}]$ .

Due to the limited water availability, evapotranspiration rates were reduced from their potential values,  $ev_{pm}$  and  $tr_{pm}$ , to their actual values,  $ev$  and  $tr$ , as approximated by the quadratic functions:

$$0.1 ev^2 - (a + ev_{pm}) ev + a \times ev_{pm} = 0, \quad (A49)$$

$$0.1 tr^2 - (b + tr_{pm}) tr + b \times tr_{pm} = 0, \quad (A50)$$

where 0.1 is the empirical convexity of the available water to the actual evapotranspiration curves;  $a$  and  $b$  are available water for evaporation and transpiration, respectively;  $a = pool_{w(1)}$ ,  $b = \sum_{i=1}^{10} \max[0, pool_{w(i)} - 0.10 \times Wwilt]$ . These equations can be transformed as follow:

$$ev = \frac{(a + ev_{pm}) - \sqrt{(a + ev_{pm})^2 - 4 \times 0.1 \times a \times ev_{pm}}}{2 \times 0.1}, \quad (A51)$$

$$tr = \frac{(b + tr_{pm}) - \sqrt{(b + tr_{pm})^2 - 4 \times 0.1 \times b \times tr_{pm}}}{2 \times 0.1}, \quad (A52)$$

Actual evaporation,  $ev$ , is charged only for top soil layer. Actual transpiration,  $tr$ , is charged for soil layers 1 to maximum *RootDepth* among existing PFT in the stand.

## Appendix B

### B1. Inputs and outputs of the SEIB–DGVM

#### Input

(1) Location

Latitude, Altitude

(2) Soil (fixed in time)

Albedo. Soil moisture at Saturation point, Field capacity, Wilting point.

(3) Climatic data (daily)

Air temperature, Soil temperature, Fraction of cloud cover, Precipitation, Humidity, Wind velocity

#### Outputs

(1) Carbon dynamics (daily–yearly)

Terrestrial carbon pool (Woody biomass, Grass biomass, Litter, Soil organic matter), CO<sub>2</sub> absorption and emission fluxes.

(2) Water dynamics (daily)

Soil moisture content (0~3mm depth at 0.1m interval), Interception rate, Evaporation rate, Transpiration rate, Interception rate, Runoff rate

(3) Radiation and heat cycles (daily)

Land surface albedo. Bowen ratio.

(4) Properties of vegetation (daily–yearly)

Biome type, Dominant plant functional type, Leaf area index, Tree density, Size distribution of trees, Age distribution of trees, Woody biomass for each tree, Grass biomass per unit area



## B2. Processes in the SEIB–DGVM, and the approaches used to represent each process

| Process                    | Approach  | Source  |
|----------------------------|---|---|
| <i>Physical process</i>    |   |   |
| Radiation                  | Beer's Law within spatially explicit virtual forest   |   |
| Evapotranspiration         | Penman–Monteith evapotranspiration  | Monteith and Unsworth (1990)                  |
| Soil water process         | Analog of simple bucket model   |   |
| <i>Physiology</i>          |   |   |
| Photosynthesis             | Michaelis-type function   |   |
| Maintenance respiration    | The respiration rate is in proportion to the nitrate content of each organ.                 | Ryan (1991)                                   |
| Growth respiration         | The respiration rate is based on the chemical composition of each organ.                    | Poorter (1994)                                |
| Stomatal conductance       | A semiempirical model   | Ball et al. (1987) modified by Leuning (1995) |
| Phenology                  | A set of semiempirical models; parameters were estimated from satellite NDVI data.          | Botta et al. (2000) except for BoNS           |
| Decomposition              | Three carbon sources: litter and soil organic carbon with slow and fast decomposition rates | Foley (1995) and Lloyd and Taylor (1994)      |
| <i>Vegetation dynamics</i> |   |   |
| Establishment              | Climatically favored PFTs establish as small individuals.                                   |   |
| Mortality                  | Annual NPP per leaf area, heat stress, bioclimatic limit, and fire                          | Sitch et al. (2003)                           |

|               |   |                        |
|---------------|---|------------------------|
| Fire          | Give by an empirical function of soil moisture and aboveground biomass  | Kistler et al. (2001)  |
| Gap formation | Give by an empirical function. This only occurs in tropical rain forest | Huth and Ditzer (2000) |

---

### B3. Parameters and constants in the model's equations

#### Fixed parameters (begins with a capital letter)

##### Soil properties (Grid specific)

|            |   |
|------------|---|
| $W_{sat}$  | : soil moisture at saturation point ( $\text{m m}^{-1}$ ) |
| $W_{fi}$   | : soil moisture at field capacity ( $\text{m m}^{-1}$ )   |
| $W_{wilt}$ | : soil moisture at wilting point ( $\text{m m}^{-1}$ )    |
| $ALBEDO$   | : soil albedo (fraction)                                  |
| $Depth$    | : depth of soil layer (= 100 mm)                          |

##### Location

|       |                     |
|-------|---------------------|
| $LAT$ | : latitude (degree) |
| $ALT$ | : altitude (m)      |

##### Allocation and Allometry (PFT-specific)

|                 |   |
|-----------------|---|
| $HGT_{max}$     | : maximum tree height (m)   |
| $HGTs$          | : initial value of relative growth rate, height to diameter ( $\text{m m}^{-1}$ )   |
| $L_{Amax}$      | : maximum leaf area per canopy surface ( $\text{m}^2 \text{m}^{-2}$ )   |
| $CD_{max}$      | : maximum crown diameter (m)  |
| $SLA$           | : specific leaf area (one sided $\text{m}^2 \text{g DM}^{-1}$ )   |
| $ALM_{1, 2}$    | : allometric parameter 1, 2 (dimensionless)   |
| $ALM_3$         | : allometric parameter 3 ( $\text{g DM m}^{-3}$ )   |
| $ALM_{4, 5, 6}$ | : allometric parameter 4, 5, 6 (fraction)   |
| $FRratio$       | : ratio of foliage mass to fine root mass for woody PFTs , and ratio of aboveground biomass to belowground biomass for grass PFTs (ratio) |

##### Respiration and turnover (PFT-specific)

|                 |  |
|-----------------|--|
| $PN_{f, s, r}$  | :nitrogen mass per biomass for foliage, sapwood, root ( $\text{g N g DM}^{-1}$ )                       |
| $RM$            | :maintenance respiration rate at 15°C for unit nitrogen mass ( $\text{g C g N}^{-1} \text{day}^{-1}$ ) |
| $RG_{f, s, r}$  | :specific growth respiration rate for foliage, sapwood, and root ( $\text{g DM g DM}^{-1}$ )           |
| $RG_{stockin}$  | :growth respiration rate from available resource to stock resource ( $\text{g DM g DM}^{-1}$ )         |
| $RG_{stockout}$ | :growth respiration rate from stock resource to available resource ( $\text{g DM g DM}^{-1}$ )         |

$TO_{f, s, r}$  :turnover rates of foliage, sapwood, and fine root for woody PFTs, while turnover rates of aboveground biomass, NA, and belowground biomass for grass PFTs ( $\text{DM}^{-1} \text{ year}^{-1}$ )

$TO_{fast, slow}$  :turnover rates for fast and slow soil organic matter (SOM) ( $\text{DM}^{-1} \text{ yr}^{-1}$ )

#### Photosynthesis (PFT-specific)

$P_{MAX}$  : maximum photosynthesis rate ( $\mu\text{mol CO}_2 \text{ m}^{-2} \text{ s}^{-1}$ )

$EK$  : light attenuation coefficient for vertical direction (dimensionless)

$LUE$  : control value of light-use efficiency for photosynthesis ( $\text{mol CO}_2 \text{ mol photon}^{-1}$ )

$T_{opt0}$  :optimum temperature for photosynthesis at very low intercellular  $\text{CO}_2$  concentration ( $^{\circ}\text{C}$ )

$T_{min}$  : minimum temperature for photosynthesis ( $^{\circ}\text{C}$ )

$T_{max}$  : maximum temperature for photosynthesis ( $^{\circ}\text{C}$ )

$GS_{b1}$  : parameters for stomatal conductance ( $\text{mol H}_2\text{O m}^{-2} \text{ s}^{-1}$ )

$GS_{b2}$  : parameters for stomatal conductance (dimensionless)

$GS_{b3}$  : parameters for stomatal conductance (hPa)

$KM$  : dependence of photosynthesis on intercellular  $\text{CO}_2$  concentration ( $\mu\text{mol mol}^{-1}$ )

$\text{CO}_2\text{cmp}$  :  $\text{CO}_2$  compensation point at  $20^{\circ}\text{C}$  ( $\mu\text{mol CO}_2 \text{ mol}^{-1} \text{ air}$ )

$\text{RootDepth}$  : Soil depth that plant can absorb soil water (10cm)

#### Establishment (PFT-specific)

$P_{establish}$  : establishment probability at vacant patch ( $\text{m}^{-2} \text{ year}^{-1}$ )

$GDD_{min}$  : minimum growth-degree-day sum ( $5^{\circ}\text{C}$  base)

$TC_{max}$  : maximum coldest-month temperature ( $^{\circ}\text{C}$ )

$PAR_{min}$  : minimum annual average of midday PAR for establishment ( $\mu\text{mol photons m}^{-2} \text{ s}^{-1}$ )

#### Mortality (PFT-specific)

$M_1$  : parameter for background mortality (dimensionless)

$M_2$  : parameter for background mortality (dimensionless)

$M_3$  : probability of survival after fire (varying 0.0–1.0)

$TC_{min}$  : minimum coldest-month temperature for survival ( $^{\circ}\text{C}$ )

#### Other fixed parameters

$ESD$  : distance between sun and earth (km)

$ESD_{mean}$  : annual mean of  $ESD$  (km)

## Variables (Begins with a lowercase letter)

### Daily climatic data

|                 |  |
|-----------------|--|
| $tmp_{air}$     | : air temperature ( $^{\circ}\text{C}$ )               |
| $tmp_{soil(i)}$ | : temperature at soil layer $i$ ( $^{\circ}\text{C}$ ) |
| $cloud$         | : total cloud cover (fraction)                         |
| $prec$          | : daily precipitation ( $\text{mm day}^{-1}$ )         |
| $humid$         | : air humidity ( $\text{g g}^{-1}$ )                   |
| $wind$          | : wind velocity ( $\text{m s}^{-1}$ )                  |

### Woody biomass (for each individual tree)

|                    |                                       |
|--------------------|---------------------------------------|
| $mass_{leaf}$      | : leaf biomass ( $\text{g DM}$ )      |
| $mass_{trunk}$     | : trunk biomass ( $\text{g DM}$ )     |
| $mass_{root}$      | : fine root biomass ( $\text{g DM}$ ) |
| $mass_{stock}$     | : stock biomass ( $\text{g DM}$ )     |
| $mass_{available}$ | : available biomass ( $\text{g DM}$ ) |

### Grass biomass

|                     |   |
|---------------------|---|
| $gmass_{leaf}$      | : leaf biomass density of grass ( $\text{g DM m}^{-2}$ )      |
| $gmass_{root}$      | : root biomass density of grass ( $\text{g DM m}^{-2}$ )      |
| $gmass_{stock}$     | : stock biomass density of grass ( $\text{g DM m}^{-2}$ )     |
| $gmass_{available}$ | : available biomass density of grass ( $\text{g DM m}^{-2}$ ) |

### Morphology and characteristics for woody PFTs (for each individual tree)

|                    |   |
|--------------------|---|
| $height$           | : tree height ( $\text{m}$ )                                  |
| $crown_{diameter}$ | : crown diameter ( $\text{m}$ )                               |
| $crown_{depth}$    | : crown depth ( $\text{m}$ )                                  |
| $crown_{area}$     | : cross sectional crown area ( $\text{m}^2$ )                 |
| $dbh_{sapwood}$    | : sapwood diameter ( $\text{m}$ )                             |
| $dbh_{heartwood}$  | : heartwood diameter ( $\text{m}$ )                           |
| $la$               | : leaf area ( $\text{m}^2$ )                                  |
| $la_{mean}$        | : annual mean leaf area in the previous year ( $\text{m}^2$ ) |

### Photosynthesis conditions

|           |   |
|-----------|---|
| $p_{ave}$ | : daily average of photosynthetic rates for each woody individual ( $\mu\text{mol}$ |
|-----------|---|

|                       |   |
|-----------------------|---|
|                       | $\text{CO}_2 \text{ m}^{-2} \text{ s}^{-1}$ )   |
| $p_{\text{sat}}$      | : light saturated photosynthetic rate ( $\mu\text{CO}_2 \text{ m}^{-2} \text{ s}^{-1}$ )  |
| $lue$                 | : light-use efficiency of photosynthesis ( $\text{mol CO}_2 \text{ mol photon}^{-1}$ )  |
| $co2_{\text{cmp}}$    | : $\text{CO}_2$ compensation point ( $\mu\text{mol CO}_2 \text{ mol air}^{-1}$ )  |
| $co2_{\text{cell}}$   | : intercellular $\text{CO}_2$ concentration ( $\mu\text{mol CO}_2 \text{ mol air}^{-1}$ )   |
| $t_{\text{opt}}$      | : optimum temperature for photosynthesis ( $^{\circ}\text{C}$ )   |
| $gs$                  | : single leaf stomatal conductance of $\text{H}_2\text{O}$ ( $\text{mol H}_2\text{O m}^{-2} \text{ s}^{-1}$ )   |
| $gs_{\text{ave}}$     | : mean daytime leaf stomatal conductance of $\text{H}_2\text{O}$ ( $\text{mol H}_2\text{O m}^{-2} \text{ s}^{-1}$ )   |
| $ccon_{\text{wood}}$  | : stomatal conductance of $\text{H}_2\text{O}$ of tree canopy, day time mean ( $\text{mol H}_2\text{O m}^{-2} \text{ s}^{-1}$ )                                 |
| $ccon_{\text{grass}}$ | : stomatal conductance of $\text{H}_2\text{O}$ of grass leaves, day time mean ( $\text{mol H}_2\text{O m}^{-2} \text{ s}^{-1}$ )                                |
| $ccon$                | : stomatal conductance of $\text{H}_2\text{O}$ , day time mean ( $=ccon_{\text{wood}} + ccon_{\text{grass}}$ , $\text{mol H}_2\text{O m}^{-2} \text{ s}^{-1}$ ) |

#### Production

|                      |   |
|----------------------|---|
| $gpp$                | : gross primary production of each tree ( $\text{g DM day}^{-1}$ )                  |
| $gpp_l$              | : gross primary production of each crown layer ( $\text{g DM day}^{-1}$ )           |
| $gpp_g$              | : gross primary production of grass layer ( $\text{g DM day}^{-1} \text{ m}^{-2}$ ) |
| $anpp$               | : annul net primary production of the previous year ( $\text{kg DM year}^{-1}$ )    |
| $stat_{\text{leaf}}$ | : benefit per cost of maintaining leaf mass ( $\text{g g}^{-1} \text{ day}^{-1}$ )  |

#### Other metabolic variables

|                       |  |
|-----------------------|--|
| $lai$                 | : leaf area index of each PFT ( $\text{m}^2 \text{ m}^{-2}$ )    |
| $lai_g$               | : leaf area index of grass layer ( $\text{m}^2 \text{ m}^{-2}$ ) |
| $stat_{\text{water}}$ | : state of water availability for each PFT (varying 0.0–1.0)     |
| $qt$                  | : temperature sensitivity of respiration                         |

#### Soil water cycle

|                      |  |
|----------------------|--|
| $prec_{\text{rain}}$ | : precipitation, rain ( $\text{mm day}^{-1}$ )                 |
| $prec_{\text{snow}}$ | : precipitation, snow ( $\text{mm day}^{-1}$ )                 |
| $rain$               | : expected number of rain in a day ( $\text{day}^{-1}$ )       |
| $pool_{w(n)}$        | : water content at soil layer $n$ ( $\text{mm}$ )              |
| $pool_{\text{snow}}$ | : water-equivalent snow depth ( $\text{mm}$ )                  |
| $tw$                 | : snowmelt rate ( $\text{mm day}^{-1}$ )                       |
| $pn_{(n)}$           | : penetration rate for soil layer $n$ ( $\text{mm day}^{-1}$ ) |

|            |  |
|------------|--|
| $ev$       | : actual evaporation rate from soil layer 1 ( $\text{mm day}^{-1}$ )       |
| $ev_{pm}$  | : potential evaporation rate from soil layer 1 ( $\text{mm day}^{-1}$ )    |
| $tr_{(n)}$ | : actual transpiration rate from soil layer $n$ ( $\text{mm day}^{-1}$ )   |
| $tr_{pm}$  | : potential transpiration rate ( $\text{mm day}^{-1}$ )                    |
| $ic$       | : intercepted rainfall by plants ( $\text{mm day}^{-1}$ )                  |
| $aet$      | : actual evapotranspiration of the previous year ( $\text{mm year}^{-1}$ ) |
| $c_{aero}$ | : aerodynamic conductance of evaporation                                   |
| $c_{soil}$ | : soil conductance of evapotranspiration                                   |
| $c_{leaf}$ | : canopy conductance of transpiration                                      |

#### Radiation conditions at midday

|                       |   |
|-----------------------|---|
| $rad_{intact}$        | : shortwave radiation at top of atmosphere ( $\text{W m}^{-2}$ )  |
| $rad$                 | : shortwave radiation entering biosphere ( $\text{W m}^{-2}$ )  |
| $rad_{direct}$        | : direct radiation within $rad$ ( $\text{W m}^{-2}$ )   |
| $rad_{diffuse}$       | : diffused radiation within $rad$ ( $\text{W m}^{-2}$ )   |
| $radnet_{veg}$        | : net radiation at vegetation surface ( $\text{W m}^{-2}$ )   |
| $radnet_{soil}$       | : net radiation at soil surface ( $\text{W m}^{-2}$ )   |
| $radnet_{long}$       | : net long wave radiation ( $\text{W m}^{-2}$ )   |
| $par$                 | : midday PAR ( $\mu\text{mol photon m}^{-2} \text{s}^{-1}$ )  |
| $par_{direct}$        | : direct radiation component of $par$ ( $\mu\text{mol photon m}^{-2} \text{s}^{-1}$ )                                 |
| $par_{diffuse}$       | : diffused radiation component of $par$ ( $\mu\text{mol photon m}^{-2} \text{s}^{-1}$ )                               |
| $par_{wood}(l, n)$    | : midday PAR on crown layer $l$ of individual tree $n$ ( $\mu\text{mol photon m}^{-2} \text{s}^{-1}$ )                |
| $par_{grass}$         | : midday PAR at the grass layer ( $\mu\text{mol photon m}^{-2} \text{s}^{-1}$ )                                       |
| $fpar_{direct}(l, n)$ | : relative intensity of direct PAR of crown disk $l$ of tree $n$ at midday compared to the forest top (dimensionless) |
| $fpar_{diffuse}(l)$   | : relative intensity of diffused of forest layer $l$ at midday compared to the forest top (dimensionless)             |
| $fpar_{direct}$       | : relative intensity of direct PAR of crown disk $l$ of tree $n$ at midday compared to the forest top (dimensionless) |
| $sl_{hgt}$            | : solar angle at midday (degree)  |
| $sl_{dec}$            | : solar declination of the Earth's orbit (degree)   |
| $dlen$                | : day length (hour)   |
| $eK$                  | : light attenuation coefficient at midday (dimensionless)   |
| $ir$                  | : shortwave interception by leaves (fraction)   |
| $albedo_{veg}$        | : albedo of vegetation surface (fraction)   |
| $albedo_{soil}$       | : albedo of soil surface (fraction)   |

**Air characteristics**

|               |  |
|---------------|--|
| $ap$          | : air pressure (hPa)   |
| $vp$          | : actual vapor pressure (hPa)  |
| $vp_{sat}$    | : saturated vapor pressure (hPa)   |
| $vpd$         | : vapor pressure deficit between saturated and actual vapor pressures (hPa)                            |
| $co2_{atm}$   | : ambient (canopy) CO <sub>2</sub> concentration ( $\mu\text{mol CO}_2 \text{ mol}^{-1} \text{ air}$ ) |
| $slope_{vps}$ | : slope of saturated vapor pressure ( $\text{hPa } ^\circ\text{C}^{-1}$ )                              |
| $dnsa$        | : density of air ( $\text{kg m}^{-3}$ )  |

**Wild fire parameters for African continent**

|                           |  |
|---------------------------|--|
| $ifire$                   | : potential fire intensity ( $\text{kJ s}^{-1} \text{ m}^{-1}$ ) |
| $\theta$                  | : fraction of fuel moisture                                      |
| $tc$                      | : fraction of tree canopy  |
| $fuel$                    | : fuel load ( $\text{gDM m}^{-2}$ )                              |
| $fuel_{living}$           | : living (moist) fuel load ( $\text{gDM m}^{-2}$ )               |
| $fuel_{dead}$             | : dead (dry) fuel load ( $\text{gDM m}^{-2}$ )                   |
| $fuel_{lying}$            | : lying dead (dry) mass ( $\text{gDM m}^{-2}$ )                  |
| $fuel_{standing}^{grass}$ | : grass standing dead (dry) mass ( $\text{gDM m}^{-2}$ )         |



B4. PFT-specific allocation and allometric parameters

| PFT   | $ALM_1$ | $ALM_2$ | $ALM_3$                 | $ALM_4$ | $ALM_5$ | $ALM_6$ | $HGT_{max}$ | $HGT_s$                 | $DBH_{limit}$ | $FR_{ratio}$ | $SLA$                             | $LA_{max}$                           | $CD_{max}$ |
|-------|---------|---------|-------------------------|---------|---------|---------|-------------|-------------------------|---------------|--------------|-----------------------------------|--------------------------------------|------------|
|       | -       | -       | (g DM m <sup>-3</sup> ) | (ratio) | (ratio) | (ratio) | (m)         | (m<br>m <sup>-1</sup> ) | (m)           | (ratio)      | (m <sup>2</sup> g <sup>-1</sup> ) | (m <sup>2</sup><br>m <sup>-2</sup> ) | (m)        |
| TrBE1 | -       | -       | 620000                  | -       | 0.2     | 0.37    | 68.0        | 140.0                   | 1.56          | 4.00         | 0.010                             | 5.0                                  | 39.0       |
| TrBE2 | -       | -       | 570000                  | -       | 0.2     | 0.28    | 68.0        | 100.0                   | 0.66          | 4.00         | 0.010                             | 5.0                                  | 16.5       |
| TrBE3 | -       | -       | 370000                  | -       | 0.2     | 0.28    | 54.0        | 95.0                    | 0.45          | 4.00         | 0.010                             | 5.0                                  | 11.3       |
| TrBE4 | -       | -       | 780000                  | -       | 0.2     | 0.28    | 42.0        | 95.0                    | 0.24          | 4.00         | 0.010                             | 5.0                                  | 6.0        |
| TrBE5 | -       | -       | 560000                  | -       | 0.1     | 0.3     | 60.0        | 172.0                   | 1.00          | 4.00         | 0.010                             | 4.0                                  | 15.0       |
| TrBR  | -       | -       | 560000                  | -       | 0.1     | 0.3     | 60.0        | 172.0                   | 1.00          | 4.00         | 0.013                             | 4.0                                  | 15.0       |
| TeNE  | 4800    | 100     | 374000                  | 0.38    | -       | -       | 43.0        | 65.0                    | 1.00          | 1.50         | 0.004                             | 4.0                                  | 15.0       |
| TeBE  | 4800    | 200     | 492000                  | 0.38    | -       | -       | 17.0        | 154.3                   | 1.00          | 1.50         | 0.007                             | 4.0                                  | 15.0       |
| TeBS  | 14500   | 200     | 492000                  | 0.20    | -       | -       | 37.0        | 159.0                   | 1.00          | 1.50         | 0.015                             | 2.0                                  | 15.0       |
| BoNE  | 6000    | 100     | 374000                  | 0.20    | -       | -       | 35.0        | 130.0                   | 1.00          | 1.50         | 0.004                             | 2.0                                  | 10.0       |
| BoNS  | 6000    | -       | -                       | -       | -       | -       | 31.7        | 165                     | 1.00          | 0.17         | 0.014                             | 4.0                                  | 8.0        |
| BoBS  | 8500    | 200     | 492000                  | 0.30    | -       | -       | 35.0        | 200.0                   | 0.4           | 1.50         | 0.016                             | 3.0                                  | 10.0       |
| TeH   | -       | -       | -                       | -       | -       | -       | -           | -                       | -             | 1.00         | 0.007                             | -                                    | -          |
| TrH   | -       | -       | -                       | -       | -       | -       | -           | -                       | -             | 0.33         | 0.007                             | -                                    | -          |

B5. PFT-specific dynamic parameters

| PFT   | $M_1$             | $M_2$             | $M_3$             | $P_{establish}$                          | $TC_{min}$ | $TC_{max}$ | $GDD_{min}$    | $PAR_{min}$   |
|-------|-------------------|-------------------|-------------------|--|------------|------------|----------------|---|
|       | (no<br>dimension) | (no<br>dimension) | (no<br>dimension) | (m <sup>-2</sup><br>year <sup>-1</sup> ) | (°C)       | (°C)       | (5 °C<br>base) | (μmol<br>photons<br>m <sup>-2</sup> s <sup>-1</sup> ) |
| TrBE1 | -                 | -                 | 0.12              | 0.020                                    | 15.5       | -          | 3000           | 20  |
| TrBE2 | -                 | -                 | 0.12              | 0.004                                    | 15.5       | -          | 3000           | 20  |
| TrBE3 | -                 | -                 | 0.12              | 0.048                                    | 15.5       | -          | 3000           | 200   |
| TrBE4 | -                 | -                 | 0.12              | 0.002                                    | 15.5       | -          | 3000           | 20  |
| TrBE5 | 0.0135            | 1.0               | 0.00              | 0.010                                    | 10.0       | -          | 3000           | 20  |
| TrBR  | 0.0135            | 1.0               | 0.00              | 0.010                                    | 10.0       | -          | 3000           | 20  |
| TeNE  | 0.018             | 1.0               | 0.12              | 0.040                                    | -2.0       | 22.0       | 900            |   |
| TeBE  | 0.008             | 1.0               | 0.50              | 0.040                                    | 3.0        | 18.8       | 1200           |   |
| TeBS  | 0.010             | 2.5               | 0.12              | 0.013                                    | -17.0      | 15.5       | 1200           |   |
| BoNE  | 0.013             | 1.2               | 0.12              | 0.005                                    | -32.5      | -2.0       | 600            |   |
| BoNS  | 0.003             | 2.0               | 0.00              | 0.013                                    | -          | -2.0       | 350            | 350   |
| BoBS  | 0.015             | 2.0               | 0.12              | 0.020                                    | -          | -2.0       | 350            | 700   |

B6. PFT-specific respiration and turnover parameters

| PFT   | $RM$  | $PN_f$                     | $RG_f$                      | $RG_s$                      | $RG_r$                      | $RG_{stockin}$              | $RG_{stocko}$               | $TO_f$                | $TO_s$                | $TO_r$                |
|-------|---|----------------------------|-----------------------------|-----------------------------|-----------------------------|-----------------------------|-----------------------------|-----------------------|-----------------------|-----------------------|
|       | (gC gN <sup>-1</sup><br>day <sup>-1</sup> ) | (gN<br>gDM <sup>-1</sup> ) | (gDM<br>gDM <sup>-1</sup> ) | (gDM<br>gDM <sup>-1</sup> ) | (gDM<br>gDM <sup>-1</sup> ) | (gDM<br>gDM <sup>-1</sup> ) | (gDM<br>gDM <sup>-1</sup> ) | (year <sup>-1</sup> ) | (year <sup>-1</sup> ) | (year <sup>-1</sup> ) |
| TrBE1 | 0.1   | 0.016                      | 1.56                        | 1.68                        | 1.34                        | 1.10                        | 1.10                        | 0.59                  | -                     | 0.76                  |
| TrBE2 | 0.1   | 0.016                      | 1.56                        | 1.68                        | 1.34                        | 1.10                        | 1.10                        | 0.59                  | -                     | 0.76                  |
| TrBE3 | 0.1   | 0.016                      | 1.56                        | 1.68                        | 1.34                        | 1.10                        | 1.10                        | 0.59                  | -                     | 0.76                  |
| TrBE4 | 0.1   | 0.016                      | 1.56                        | 1.68                        | 1.34                        | 1.10                        | 1.10                        | 0.59                  | -                     | 0.76                  |
| TrBE5 | 0.1   | 0.016                      | 1.56                        | 1.68                        | 1.34                        | 1.10                        | 1.10                        | 0.59                  | -                     | 0.59                  |
| TrBR  | 0.1   | 0.022                      | 1.56                        | 1.68                        | 1.34                        | 1.10                        | 1.10                        | 1.59                  | -                     | 1.59                  |
| TeNE  | 0.1   | 0.012                      | 1.56                        | 1.68                        | 1.34                        | 1.10                        | 1.10                        | 0.22                  | 0.05                  | 0.64                  |
| TeBE  | 0.1   | 0.012                      | 1.56                        | 1.68                        | 1.34                        | 1.10                        | 1.10                        | 0.38                  | 0.05                  | 0.64                  |
| TeBS  | 0.1   | 0.022                      | 1.56                        | 1.68                        | 1.34                        | 1.10                        | 1.10                        | 2.17                  | 0.05                  | 0.64                  |
| BoNE  | 0.1   | 0.012                      | 1.56                        | 1.68                        | 1.34                        | 1.10                        | 1.10                        | 0.22                  | 0.05                  | 0.42                  |
| BoNS  | 0.1   | 0.016                      | 1.56                        | 1.68                        | 1.34                        | 1.10                        | 1.10                        | 4.00                  | -                     | 0.16                  |
| BoBS  | 0.1   | 0.025                      | 1.56                        | 1.68                        | 1.34                        | 1.10                        | 1.10                        | 3.33                  | 0.05                  | 0.42                  |
| TeH   | 0.1   | 0.027                      | 1.50                        | -                           | 1.34                        | 1.10                        | 1.10                        | 3.19                  | -                     | 0.40                  |
| TrH   | 0.1   | 0.018                      | 1.50                        | -                           | 1.34                        | 1.10                        | 1.10                        | 0.5                   | -                     | 0.77                  |

B7. PFT-specific photosynthesis parameters

| PFT   | $P_{MAX}$  | $EK$         | $LUE$   | $T_{opt0}$             | $T_{min}$              | $T_{max}$              | $GS_{b1}$  | $GS_{b2}$    | $GS_{b3}$ | $KM$                         | $CO2_{cmp}$   | $RootDepth$              |
|-------|--|--------------|---|------------------------|------------------------|------------------------|--|--------------|-----------|------------------------------|---|--------------------------|
|       | ( $\mu\text{mol CO}_2 \text{ m}^{-2} \text{ s}^{-1}$ ) | no dimension | ( $\text{mol CO}_2 \text{ mol photon}^{-1}$ ) | ( $^{\circ}\text{C}$ ) | ( $^{\circ}\text{C}$ ) | ( $^{\circ}\text{C}$ ) | ( $\text{mol H}_2\text{O m}^{-2} \text{ s}^{-1}$ ) | no dimension | (hPa)     | ( $\mu\text{mol mol}^{-1}$ ) | ( $\mu\text{mol CO}_2 \text{ mol}^{-1} \text{ air}$ ) | ( $\times 10\text{cm}$ ) |
| TrBE1 | 9.4  | 0.50         | 0.10  | 27.5                   | 2.0                    | 47.5                   | 0.01   | 5.0          | 10.0      | 33.0                         | 50.0  | 5                        |
| TrBE2 | 9.9  | 0.50         | 0.06  | 27.5                   | 2.0                    | 47.5                   | 0.01   | 5.0          | 10.0      | 33.0                         | 50.0  | 5                        |
| TrBE3 | 26.0   | 0.50         | 0.06  | 27.5                   | 2.0                    | 47.5                   | 0.01   | 5.0          | 10.0      | 33.0                         | 50.0  | 5                        |
| TrBE4 | 16.3   | 0.50         | 0.09  | 27.5                   | 2.0                    | 47.5                   | 0.01   | 5.0          | 10.0      | 33.0                         | 50.0  | 5                        |
| TrBE5 | 8.1  | 0.50         | 0.05  | 27.5                   | 2.0                    | 47.5                   | 0.01   | 5.0          | 10.0      | 33.0                         | 50.0  | 5                        |
| TrBR  | 11.9   | 0.50         | 0.05  | 27.5                   | 2.0                    | 47.5                   | 0.01   | 5.0          | 10.0      | 30.0                         | 50.0  | 5                        |
| TeNE  | 9.0  | 0.50         | 0.05  | 25.0                   | 0.0                    | 45.0                   | 0.01   | 5.0          | 10.0      | 30.0                         | 50.0  | 5                        |
| TeBE  | 9.0  | 0.50         | 0.05  | 25.0                   | 0.0                    | 45.0                   | 0.01   | 5.0          | 10.0      | 30.0                         | 50.0  | 5                        |
| TeBS  | 12.0   | 0.50         | 0.05  | 22.5                   | -2.0                   | 42.5                   | 0.01   | 5.0          | 10.0      | 30.0                         | 50.0  | 5                        |
| BoNE  | 9.3  | 0.50         | 0.05  | 18.0                   | -4.0                   | 38.5                   | 0.01   | 5.0          | 10.0      | 30.0                         | 50.0  | 5                        |
| BoNS  | 13.0   | 0.50         | 0.05  | 20.0                   | 5.0                    | 35.0                   | 0.01   | 5.0          | 10.0      | 30.0                         | 50.0  | 5                        |
| BoBS  | 9.0  | 0.50         | 0.05  | 18.0                   | -4.0                   | 38.5                   | 0.01   | 5.0          | 10.0      | 35.0                         | 50.0  | 5                        |
| TeH   | 8.0  | 0.50         | 0.05  | -                      | -1.0                   | 45.0                   | 0.01   | 5.0          | 10.0      | 37.0                         | 50.0  | 2                        |
| TrH   | 12.0   | 0.50         | 0.05  | -                      | 2.5                    | 55.0                   | 0.01   | 2.0          | 10.0      | 10.0                         | 5.0   | 10                       |

B9. Classification scheme of vegetation type, taken from Haxeltine and Prentice (1996) with some simplifications and modifications.

| Vegetation type conditions     | Dominant PFT                 | Other                |
|--------------------------------|------------------------------|----------------------|
| <b>Group 1</b>                 |                              |                      |
| Desert (polar)                 | any                          | $GDD_0 < 150$        |
| <b>Group 2</b>                 |                              |                      |
| Arctic / Alpine-tundra         | any                          | $GDD_5 < 370$        |
| <b>Group 3</b>                 |                              |                      |
| Tropical forest                | TrBE                         | $2.5 \leq LAI_{max}$ |
| Tropical deciduous forest      | TrBR                         | $2.5 \leq LAI_{max}$ |
| Temperate evergreen forest     | TeNE                         | $1.5 \leq LAI_{max}$ |
| Temperate evergreen forest     | TeBE                         | $3.0 \leq LAI_{max}$ |
| Temperate deciduous forest     | TeBS                         | $2.5 \leq LAI_{max}$ |
| Boreal evergreen forest        | BoNE                         |                      |
| Boreal deciduous forest        | BoNS or BoBS                 |                      |
| <b>Group 4</b>                 |                              |                      |
| Xeric wood-land / scrub        | Tropical woody or TeBE       | $1.0 \leq LAI_{max}$ |
|                                | Boreal woody or TeNE or TeBS | $1.5 \leq LAI_{max}$ |
| <b>Group 5</b>                 |                              |                      |
| Grass land / Savannas / Steppe | any                          | $0.2 \leq LAI_{max}$ |
| Desert (arid)                  | any                          | $LAI_{max} < 0.2$    |

Note: Priority of classification: Group 1 > Group 2 > Group 3 > Group 4 > Group 5,  $GDD_0$ : growing-degree-day at 0 °C base,  $GDD_5$ : growing-degree-day at 5 °C base,  $LAI_{max}$ : maximum leaf area index of the previous year ( $m^2 m^{-2}$ )

## Literature cited

- Archibald, S., D. P. Roy, B. W. van Wilgen, and R. J. Scholes (2009), What limits fire? An examination of drivers of burnt area in Southern Africa, *Global Change Biol.*, 15(3), 613-630.
- Arora, V.K., Boer, G.J., 2005. A parameterization of leaf phenology for the terrestrial ecosystem component of climate models. *Global Change Biol.* 11, 39-59.
- Ball, J.T., Woodrow, I.E., Berry, J.A., 1987. A model predicting stomatal conductance and its contribution to the control of photosynthesis under different environmental conditions. In: Biggens, J. (Ed.), *Progress in Photosynthesis Research*. Martinus Nijhoff Publishers, Dordrecht, pp. 221-224.
- Botta, A., Viovy, N., Ciais, P., Friedlingstein, P., Monfray, P., 2000. A global prognostic scheme of leaf onset using satellite data. *Global Change Biol.* 6, 709-725.
- Brooks, A., Farquhar, G.D., 1985. Effect of temperature on the CO<sub>2</sub>/O<sub>2</sub> specificity of ribulose-1,5-bisphosphate carboxylase oxygenase and the rate of respiration in the light - Estimates from gas-exchange measurements on Spinach. *Planta* 165, 397-406.
- Collatz, G.J., Berry, J.A., Clark, J.S., 1998. Effects of climate and atmospheric CO<sub>2</sub> partial pressure on the global distribution of C-4 grasses: present, past, and future. *Oecologia* 114, 441-454.
- FAO, 1991. The Digitized Soil Map of the World (Release 1.0). In, Food and Agriculture Organization of the United Nations.
- FFPRI (Forestry and Forest Products Research Institute), Viewed October 27 2004, 2003.
- Foley, J.A., 1995. An equilibrium-model of the terrestrial carbon budget. *Tellus Series B-Chemical and Physical Meteorology* 47, 310-319.
- Friend, A.D., Stevens, A.K., Knox, R.G., Cannell, M.G.R., 1997. A process-based, terrestrial biosphere model of ecosystem dynamics (Hybrid v3.0). *Ecol. Model.* 95, 249-287.
- Gill, R.A., Jackson, R.B., 2000. Global patterns of root turnover for terrestrial ecosystems. *New Phytol.* 147, 13-31.
- Haxeltine, A., Prentice, I.C., 1996. BIOME3: An equilibrium terrestrial biosphere model based on ecophysiological constraints, resource availability, and competition among plant functional types. *Global Biogeochemical Cycles* 10, 693-709.

Higgins, S. I., W. J. Bond, and W. S. W. Trollope (2000) Fire, resprouting and variability: a recipe for grass-tree coexistence in savanna, *J. Ecol.*, 88(2), 213-229.

Huth, A., Ditzer, T., 2000. Simulation of the growth of a lowland Dipterocarp rain forest with FORMIX3. *Ecol. Model.* 134, 1-25.

Huth, A., Ditzer, T., Bossel, H., 1998. The rain forest growth model FORMIX3 - Model description and analysis of forest growth and logging scenarios for the Deramakot forest reserve (Malaysia). Erich Goltze, GoEttingen.

Ito, A., Oikawa, T., 2002. A simulation model of the carbon cycle in land ecosystems (Sim-CYCLE): a description based on dry-matter production theory and plot-scale validation. *Ecol. Model.* 151, 143-176.

Jones, H.G., 1992. Radiation. In, *Plants and microclimate*. Cambridge University press, pp. 9-44.

Kistler, R., Kalnay, E., Collins, W., Saha, S., White, G., Woollen, J., Chelliah, M., Ebisuzaki, W., Kanamitsu, M., Kousky, V., van den Dool, H., Jenne, R., Fiorino, M., 2001. The NCEP-NCAR 50-year reanalysis: monthly means CD-ROM and documentation. *Bull. Am. Meteorol. Soc.* 82, 247-267.

Kohler, P., 1998. Parameter research for the tropical rain forest model FORMIX4. In, Research report P9801, Center for Environmental Systems Research, University of Kassel, Germany. University of Kassel.

Koppen, W. 1936. Das geographische System der Klimate (Handbuch der Klimatologie, Bd. 1, Teil C).

Kuroiwa, S., 1979. Population photosynthesis. In: Iwajyo, H. (Ed.), *Population photosynthesis. Function and Productivity of Plant Population*. Asakura-shoten, Tokyo, pp. 84-141 (in Japanese).

Lambers, H., Chapin, F.S., Pons, T.L., 1998. *Plant Physiological Ecology*. Springer, New-York.

Larcher, W., 1995. *Physical plant ecology*. Springer, Berlin.

Leuning, R., 1995. A critical-appraisal of a combined stomatal-photosynthesis model for C-3 plants. *Plant Cell and Environment* 18, 339-355.

Lloyd, J., Taylor, J.A., 1994. On the temperature dependence of soil respiration. *Funct. Ecol.* 8,

313-323.

Monteith, J.L., Unsworth, M.H., 1990. *Principles of Environmental Physics*. Arnold Press, London.

Neilson, R.P., 1995. A model for predicting continental-scale vegetation distribution and water-balance. *Ecol. Appl.* 5, 362-385.

Osmond, C.B., Bjorkman, O., Anderson, D.J., 1980. In, *Photosynthesis Physiological Processes in Plant Ecology*. Springer-Verlag, Berlin, pp. 291-377.

Penman, H.L., 1948. Natural evaporation from open water, bare soil and grass. *Proceedings of the Royal Society London, series A* 193, 120-145.

Penning de Vries, F.W.T., 1973. Use of assimilates in higher plants. In: Cooper, J.P. (Ed.), *Photosynthesis and productivity in different environments*. Cambridge Univ. Press, pp. 459-480.

Picard, G., Quegan, S., Delbart, N., et al. 2005. Bud-burst modelling in Siberia and its impact on quantifying the carbon budget. *Global Change Biol.* 11, 2164-2176.

Pooter, H., 1994. Construction costs and payback time of biomass: A whole plant perspective. In: Roy, J., Garnier, E. (Eds.), *A whole plant perspective on carbon-nitrogen interactions*. SPB Academic, Hague, Netherlands.

Raich, J.W., Rastetter, E.B., Melillo, J.M., et al. 1991. Potential net primary productivity in South America: application of a global model. *Ecol. Appl.* 1, 399-429.

Reich, P.B., Walters, M.B., Ellsworth, D.S., 1997. From tropics to tundra: Global convergence in plant functioning. *Proc. Natl. Acad. Sc. USA* 94, 13730-13734.

Rosenberg, N. J., B. L. Blad, and S. B. Verma (1983) *Evaporation and Evapotranspiration, in Microclimate: The Biological Environment*, edited, pp. 209-287, Wiley-Interscienc.

Ryan, M.G., 1991. Effects of climate change on plant respiration. *Ecol. Appl.* 1, 157-167.

Sato, H., 2009. Simulation of the vegetation structure and function in a Malaysian tropical rain forest using the individual-based dynamic vegetation model SEIB-DGVM, *Forest Ecology and Management*. For. Ecol. Manage. 257, 2277-2286.

Sato, H., Itoh, A., Kohyama, T., 2007. SEIB-DGVM: A new dynamic global vegetation model using a spatially explicit individual-based approach. *Ecol. Model.* 200, 279-307.



Sato, H., Kobayashi, H., Delbart, N., 2009. Simulation study of the vegetation structure and function in eastern Siberian larch forests using the individual-based vegetation model SEIB-DGVM. *For. Ecol. Manage.*

Scheiter, S., and S. I. Higgins (2009) Impacts of climate change on the vegetation of Africa: an adaptive dynamic vegetation modelling approach, *Global Change Biol.*, 15(9), 2224-2246.

Schulze, E.D., Schulze, W., Kelliher, F.M., et al. 1995. Aboveground biomass and nitrogen nutrition in a chronosequence of pristine Dahurian *Larix* stands in eastern Siberia. *Canadian Journal of Forest Research-Revue Canadienne de Recherche Forestiere* 25, 943-960.

Shinozaki, K., Yoda, K., Hozumi, K., Kira, T., 1964a. A quantitative analysis of plant form, The pipe model theory I. *Jpn. J. Ecol.* 14, 97-105.

Shinozaki, K., Yoda, K., Hozumi, K., Kira, T., 1964b. A quantitative analysis of plant form, The pipe model theory II: Further evidence of the theory and its application in forest ecology, *Jpn. J. Ecol.* 14, 133-139.

Sitch, S., Smith, B., Prentice, I.C., et al., 2003. Evaluation of ecosystem dynamics, plant geography and terrestrial carbon cycling in the LPJ dynamic global vegetation model. *Global Change Biol.* 9, 161-185.

Thonicke, K., Venevsky, S., Sitch, et al. 2001. The role of fire disturbance for global vegetation dynamics: coupling fire into a Dynamic Global Vegetation Model. *Global Ecol. Biogeogr.* 10, 661-677.

van Wilgen, B., and R. Scholes (1997) The vegetation and fire regimes of southern hemisphere Africa, in *Fire in African Savannas*, edited, pp. 27-46, Witwatersrand University Press, Johannesburg, South Africa.

Warning, R.H., 1983. Estimating forest growth and efficiency in relation to canopy leaf area. *Adv. Ecol. Res.* 13, 327-354.

Wright, I.J., Reich, P.B., Westoby, M., et. al. 2004. The worldwide leaf economics spectrum. *Nature* 428, 821-827.

Yokota, T., Hagihara, A., 1996. Seasonal change in the temperature coefficient Q<sub>10</sub> for respiration of field-grown hinoki cypress (*Chamaecyparis obtusa*) trees. *Journal of Forest Research* 1, 165-168.

Zeide, B., 2001. Natural thinning and environmental change: an ecological process model. *For. Ecol. Manage.* 154, 165-177.

Zobler, L., 1986. A world soil file for global climate modeling. NASA Technical Memorandum, 87802, 1-32.

# Figures

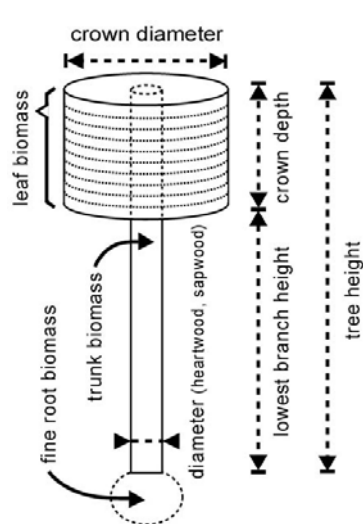


Figure 1

Representation of individual trees in the SEIB–DGVM. Each tree is composed of a crown, trunk, and fine roots. The trunk is composed of heartwood and sapwood. Trunk biomass includes branches and coarse/tap roots. The crown consists of 10-cm-deep ‘disks’. The trunk and the crown both have cylindrical shapes, while the fine roots are formless (i.e., represented only by biomass).

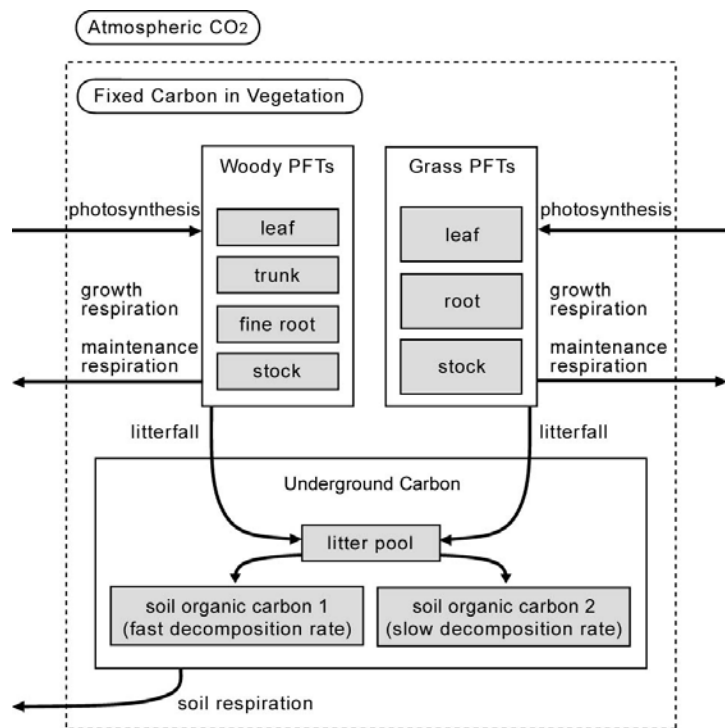


Figure 2

The carbon flow through a terrestrial ecosystem as simulated by the SEIB–DGVM.

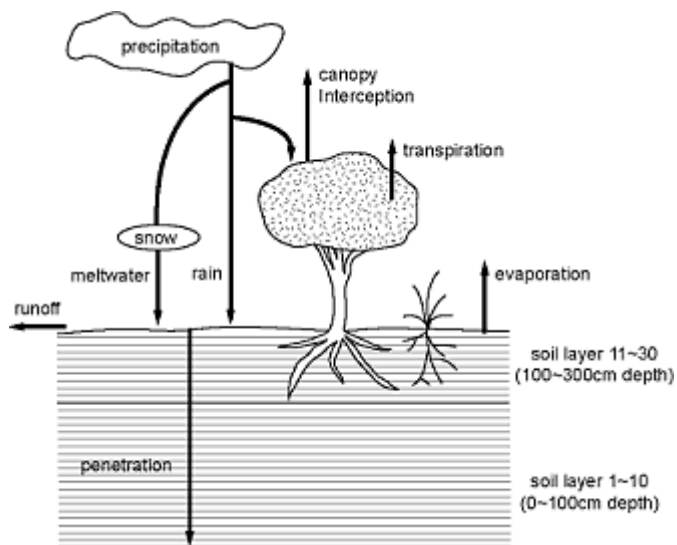


Figure 3

The water flow through the terrestrial ecosystem as simulated by the SEIB-DGVM.

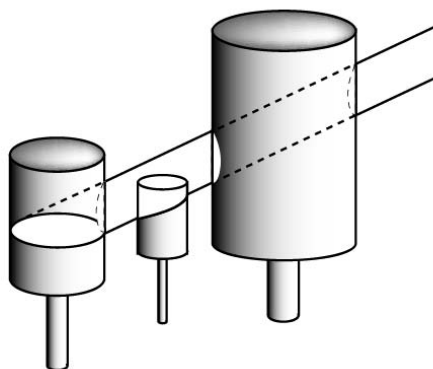


Figure 4

Schematic diagram of how to allocate direct radiation among trees in the SEIB-DGVM. See text for explanation.